Geological Magazine

www.cambridge.org/geo

Shales of Palaeo-Mesoproterozoic Vindhyan Basin, central India: insight into sedimentation dynamics of Proterozoic shelf

Arvind K. Singh[1] and Partha Pratim Chakraborty[2,3]

[1]Birbal Sahni Institute of Palaeosciences, 53 University Road, Lucknow 226007, India; [2]Department of Geology, University of Delhi, New Delhi 110007, India and [3]Hiroshima Institute of Plate Convergence Region Research, Hiroshima University, Higashi–Hiroshima 7398526, Japan

Review Article

Cite this article: Singh AK and Chakraborty PP (2022) Shales of Palaeo-Mesoproterozoic Vindhyan Basin, central India: insight into sedimentation dynamics of Proterozoic shelf. *Geological Magazine* **159**: 247–268. https://doi.org/10.1017/S0016756820001168

Received: 16 May 2020
Revised: 20 September 2020
Accepted: 23 September 2020
First published online: 23 November 2020

Keywords:
Vindhyan Basin; shale; Mesoproterozoic; sedimentation dynamics; Proterozoic shelf

Author for correspondence:
Partha Pratim Chakraborty,
Email: parthageology@gmail.com

Abstract

The Vindhyan Supergroup represents the largest Proterozoic sedimentary basin fill in the Indian shield. In addition to some significant palaeobiological discoveries, the sedimentary sequence of the Vindhyan, particularly its argillaceous intervals, holds crucial information for our understanding of sedimentation dynamics in Proterozoic clastic shelves. Here we attempt an extensive, although not exhaustive, review of the physical characteristics of six argillaceous (shale) intervals (Arangi, Koldaha, Rampur, Bijaygarh, Rewa and Sirbu shale) from the Son valley sector, Vindhyan Basin, augmented with new observations to unravel the status of current understanding in terms of palaeo-flow dynamics, shelf sedimentation processes and dispersal pattern, depositional cyclicity and basinal tectonics. The sedimentary attributes of Vindhyan shales reveal their deposition largely in relative bathymetry fluctuating from distal shoreface or inner shelf (near to fair-weather wave base) to distal shelf below storm wave base. More often than not, the Vindhyan shelf was storm-infested and the operation of both storm-generated return flow and Coriolis-force-guided geostrophic currents are documented from different stratigraphic intervals of argillaceous successions. The thick arenaceous intervals interrupting the deposits of the Koldaha, Rewa and Sirbu shales at multiple stratigraphic levels indicate the presence of a fan delta and braided fluvial system during intermittent regressive stands of sea level or event deposition during a sea-level highstand, respectively. Based on facies pattern and flow vectors, a rift-related half-graben model is inferred for Arangi and Koldaha shale and a low-gradient stable-shelf model with well-defined energy gradient is proposed for successions from Rampur shale onwards.

1. Introduction

Among the different varieties of sedimentary rocks, namely clastic, chemical and organo-chemical, shales are the most abundant worldwide (> 70% of sedimentary cover) and are traditionally considered suitable for understanding the nature, scale, heterogeneity and physical sedimentation parameters in low-energy depositional environments. Constituted dominantly of clays, transported in suspension, and subordinately of silt/sand, shales record significant clues on operative depositional processes in ancient shelves. Shales also provide a signature of sediment provenance and basin tectonics, thereby complementing inferences drawn from studies on sandstones and carbonates (Schieber, 1986, 1989, 1990, 1991; Sarkar *et al.* 2002*a*, *b*; Potter *et al.* 2005; Kasanzu *et al.* 2008; Srivastava *et al.* 2018). The generation of mud is dependent on climate, lithology and the relief of the source area, and, once produced, is redistributed by slides, slumps, mass flows and currents (terrestrial and basinal) at different scales. It is generally believed that low settling velocity and flocculation allow even weak currents to disperse clay-sized particles over large areas; it has also been argued from recent flume studies (Schieber, 2016) that flocculated mud can be transported by currents able to move bedload sand. This new understanding has brought shale sedimentology to the forefront; what was previously interpreted as a deep stagnant environment from laminated shale successions may possibly now be interpreted as belonging to an energetic and dynamic depositional environment. Careful studies of marine shale successions have revealed evidence of the operation of close-spaced multidirectional events such as distal tidal currents, storm-wave impingement and unidirectional currents (bottom flow, turbidites) on the muddy sea floor. In this backdrop, it is important to emphasize that the study of argillaceous formations present in the rock record can provide geological information to improve knowledge of issues that is are either very poorly understood or so far unaddressed. However, sedimentologists generally treated shale formations briefly, neglecting the geological information obtainable from sub-microscopic grain sizes and lithological homogeneity. Process-related facies analysis in terms of physical characteristics of shales is seldom carried out (e.g. Schieber, 1986; Sarkar *et al.* 2002*a*).

CAMBRIDGE UNIVERSITY PRESS

We therefore focus on the argillaceous intervals of the Palaeo-Mesoproterozoic Vindhyan Basin, central India, which records a sedimentation history of > 500 Ma (>1631 ± 5 Ma (Ray *et al.* 2002) to 1000 Ma (Malone *et al.* 2008)), spanning the period of Earth's history that included drastic and irreversible changes in the lithosphere, hydrosphere, atmosphere and biosphere. We attempt a synthesis of the physical characteristics of six different argillaceous (shale) intervals (Arangi, Koldaha, Rampur, Bijaygarh, Rewa and Sirbu) from the Vindhyan Supergroup exposed within the Son valley sector. From the collation of data generated in this study along with available data in literature, we have attempted to summarize the current understanding in terms of palaeo-flow dynamics, sediment dispersal pattern, depositional setting and cyclicity, and basin tectonics.

2. Geological setting and stratigraphic framework

The cratonic Proterozoic sedimentary basins of India are comparable with the Proterozoic basins of North America, Australia and the Siberian platform with respect to age, duration of basin history, size, sediment thickness and depositional systems (Preiss & Forbes, 1981; Kale & Phansalkar, 1991; Patranabis-Deb, 2004; Wani & Mondal, 2011). The Vindhyan Basin, hosted within the Bundelkhand Craton (3.3–2.5 Ga; Crawford & Compston, 1969; Mondal *et al.* 2002) and exposed over an area of 178 000 km^2 (Tandon *et al.* 1991), represents the largest Proterozoic basin of India; it consists of an approximately 4500-m-thick mixed siliciclastic–carbonate package that is deformed and unmetamorphosed (Fig. 1a, b). The basin is bound by the Aravalli–Delhi orogenic belt (2500–900 Ma; Roy, 1988) in the west and the Satpura orogen (1600–850 Ma; Verma, 1991) in the south and east. The Bundelkhand granite massif occurs at the centre of the basin and divides it into two sub-basins: the Son Valley Vindhyans in the east and the Rajasthan Vindhyans to the west (Fig. 1a). Much of the northern part of the basin, along with the Aravalli–Delhi fold belt and the Bundelkhand granite gneiss, is overlain by recent Gangetic alluvium. The southern part of the Vindhyan Basin is covered by Deccan lava (Krishnan, 1968), and its edge is marked by a major structural lineament known as the Narmada–Son Lineament. It is agreed that, subsequent to the stabilization of the Aravalli–Bhandara craton with a post-orogenic granitic intrusion at *c.* 2.5 Ga (Eriksson *et al.* 1999; Roger *et al.* 1999), the craton thickness reduced as a result of continued rifting. These rifts accommodated sediments of early Proterozoic age, such as the Gwalior, Bijawar and Mahakoshal groups (Mazumder *et al.* 2000; Bose *et al.* 2001; Chakraborty *et al.* 2015). Unconformably overlying early riftogenic sediments, the Vindhyan Supergroup occurs as a largely undeformed sediment package, dominated by immature siliciclastics and carbonate-rich sediments in its lower part and mature siliciclastics in its upper part. The Supergroup is subdivided into two groups – the Lower Vindhyan (Semri Group) and Upper Vindhyan (Kaimur, Rewa and Bhander) – separated by a basin-wide unconformity and its correlative conformity (Bose *et al.* 2015; Mandal *et al.* 2019; Fig. 1b).

3. Vindhyan shales

Six argillaceous formations of the Vindhyan Supergroup, covering nearly the entire sedimentation history of the basin with variegated facies development, are used for documenting depositional processes, depositional cyclicity and sediment dynamics. Since the argillaceous successions are repeatedly intercepted by coarser clastic intervals at different stratigraphic levels, the coarser clastic intervals are also discussed here to highlight spatio-temporal variations in depositional parameters on muddy shelves in response to different allokinetic or autokinetic triggers. Further, the proliferation of algal mats significantly influenced the sedimentation on the Vindhyan shelf, including shaping and/or morphing the bedforms, and is therefore considered to be important in shale sedimentology (Sarkar *et al.* 2014).

The three lower Vindhyan shales (Arangi, Koldaha and Rampur) are described in Sections 3.a–3.c, and the three upper Vindhyan shales (Bijaygarh, Rewa and Sirbu) are described in Sections 3.d–3.e below.

3.a. Arangi shale

Overlying the conglomerates and coarse-grained sandstones of the Deoland Formation, the Arangi shale (70–200 m) forms the lowermost shale interval in the Vindhyan sediment package. Because of extremely poor exposure, characterization of this shale unit is very sketchy and mostly described as greenish-grey to dark-grey shale with khaki siltstones and fine sandstones (Singh, 1973; Gupta *et al.* 2003). Gupta *et al.* (2003) reported coaly matter and pyrite disseminations from wave-rippled and flaser-bedded fine sandy interbeds present within the black carbonaceous to porcellanitic shale. We sampled a section of Arangi shale approximately 1.8 m thick exposed at the Dalla cement factory, Dalla, Uttar Pradesh (Fig. 2a). In contrast to previously reported lithology, the dominant lithology is marked by dark-grey to black fissile shale punctuated by millimetre-thick silt interbeds, rich in feldspar. The silt interbeds are laterally discontinuous, have sharp contacts with encasing shale, and are internally massive or plane laminated (Fig. 2a). The shale beds do not reveal the presence of any wave or current feature. Interestingly, samples from this shale unit have yielded very high (3.6–8.4%) total organic carbon (TOC) values.

Upwards, the Arangi shale gradationally passes to the Kajrahat limestone; a limestone–shale heterolithic succession marks the transition (Fig. 2b). The limestone (calcarenite) interbeds within the heterolithic package have a sharp and, more often than not, erosional contact with underlying black shales, but there is a gradational contact with overlying shales (Fig. 2b(iv)). Often, soles of the calcarenite beds are marked with small flute casts which are found as loaded and record a northwesterly palaeoflow azimuth (Fig. 2b(ii)). Internally, these beds are either plane laminated or wavy laminated with laminae having a centripetal dip, thereby mimicking micro-hummocky structure (Fig. 2b(iii)). Interbedded shale units are black in colour, fissile and pyritiferous. Millimetre-thick stringers of pyrite can be observed paralleling laminations of shale. Higher upwards, the heterolithic limestone–shale packages are found in alternation with metre-thick bedded algal-laminated limestone units (Fig. 2b(i)). AK Singh (unpub. PhD thesis, University of Delhi, 2015) identified two orders of cyclicity in the shale-rich basal succession, namely: (1) cyclic alternation between limestone and shale; and (2) alternation between heterolithic facies and amalgamated algal laminite bedsets.

3.a.1. Sedimentation and depositional environment

The lack of any current or wave feature, including a storm signature, favour deposition of this dark-grey shale succession distally offshore below the storm wave base (Bose *et al.* 1997; Eriksson *et al.* 1998; Sarkar *et al.* 2002*a*). Thin silt interbeds with sharp non-erosional contact with encasing shale are interpreted as products of plume deposition in a distal shelf environment, supplied

https://doi.org/10.1017/S0016756820001168 Published online by Cambridge University Press

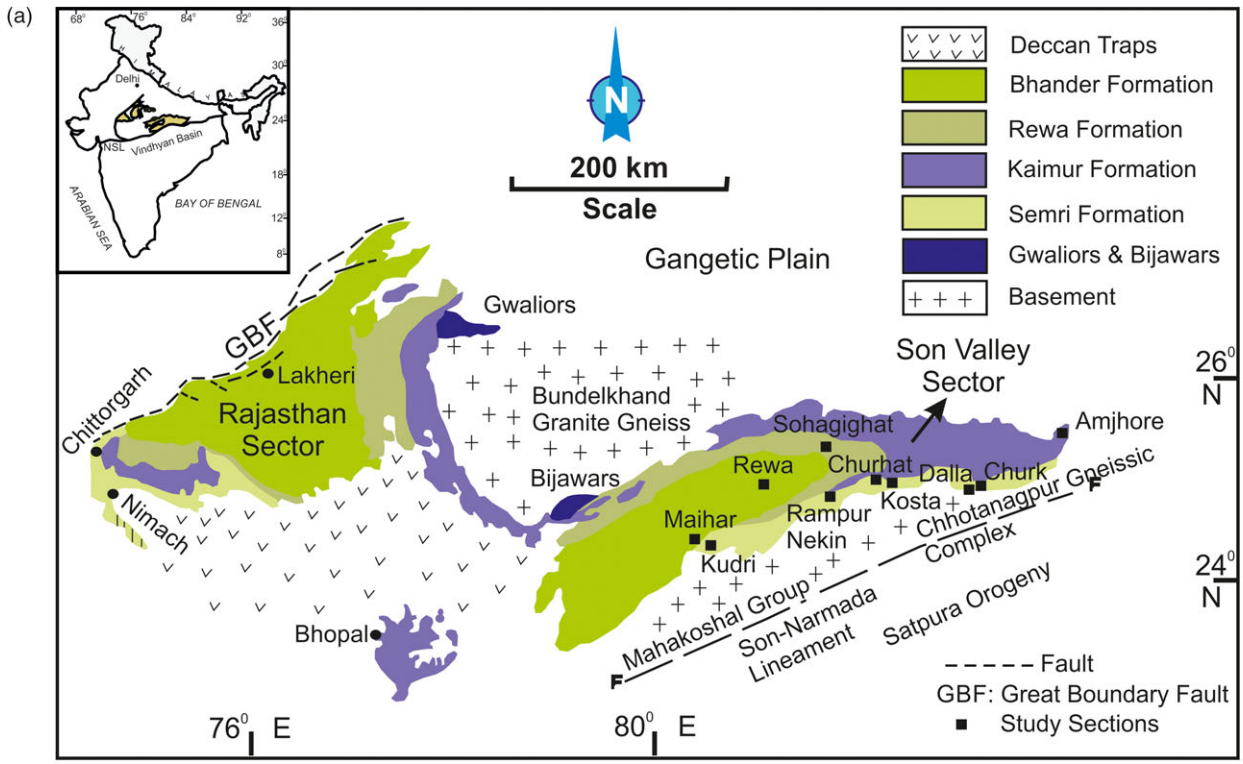

(b)

Vindhyan Succession (Son Valley)			Litholog	Description	Operative Processes	Paleogeography	Age
VINDHYAN SUPERGROUP	Upper Vindhyan Group	BHANDER	Upper Bhander Sst.				*c.* 1000 Ma U–Pb (MC-ICPMS)
			Sirbu Shale	Carbonate interbeds in Sh. below;Sst-Sh interbeds increasing Sst-Sh ratio above	Geostrophic current, storm return flow & turbiditic flow	Lagoonal, outer to inner shelf towards top	>1000 Ma (?)
			Lower Bhander Sst.				
			Bhander Lst.				
			Ganurgarh Sh.				
		REWA	Rewa Sst.				
			Rewa Shale	Sst-Sh alternation with hummocks & wave feature	Storm return flow	Outer to inner shelf	1100-700 Ma (Chuaria-Tawuia)
		KAIMUR	Upper Sst.				
			Bijaygarh Shale	Black sh. & sst-sh heterolithic unit with wave & sole features	Storm return flow, Geostrophic current	Anoxic, distal to inner shelf	1210±52 Ma (Re–Os)
			Lower Sst.				
	Lower Vindhyan Group (Semri)	ROHTAS	Rohtas Lst.				
			Rampur Shale	Greenish grey to black sh. with large width gutters	Storm return flow	Inner to outer shelf setting in sag tectonics	1599±8 Ma (U–Pb-SHRIMP)
		KHIENJUA	Churhat Sst.				
			Koldaha Shale	Sh-sst alternation. Poorly sorted coarse sst. Thickening- and thinning-upwards packages	Storm return flow, Turbiditic flow	Distal to proximal shelf, Prodelt-aic setting in half-graben set-up	
		PORCELLANITE					1628±8 Ma (U–Pb-SHRIMP)
		KAJRAHAT	Kajrahat Lst.	Alternate Lst-black sh. hetrolithic basal unit	Storm-induced flow on carbonate platform	Distal to proximal shelf in half-graben set-up	1721±90 (Pb-Pb)
			Arangi Shale	Poorly exposed greenish to dark grey shale with Khaki siltstones	No wave or current process. Plume deposition of silt	Distal offshore in half-graben set-up	
		DEOLAND					

Sandstone | Black Shale | Grey Shale | Volcaniclastics | Carbonate | Lamproite pipe

Fig. 1. (a) Geological map of the Vindhyan basin (modified after Krishnan & Swaminath, 1959) with locations of study area. (b) Stratigraphy of the Vindhyan Supergroup exposed at the Son Valley highlighting the studied shale intervals (bright green) with physical characteristics, operative processes, palaeogeography and available isotopic dates. Lst. – limestone; MC-ICPMS – multicollector inductively coupled plasma mass spectrometry; Sh. – shale; Sst. – sandstone; SHRIMP – sensitive high-resolution ion microprobe.

https://doi.org/10.1017/S0016756820001168 Published online by Cambridge University Press

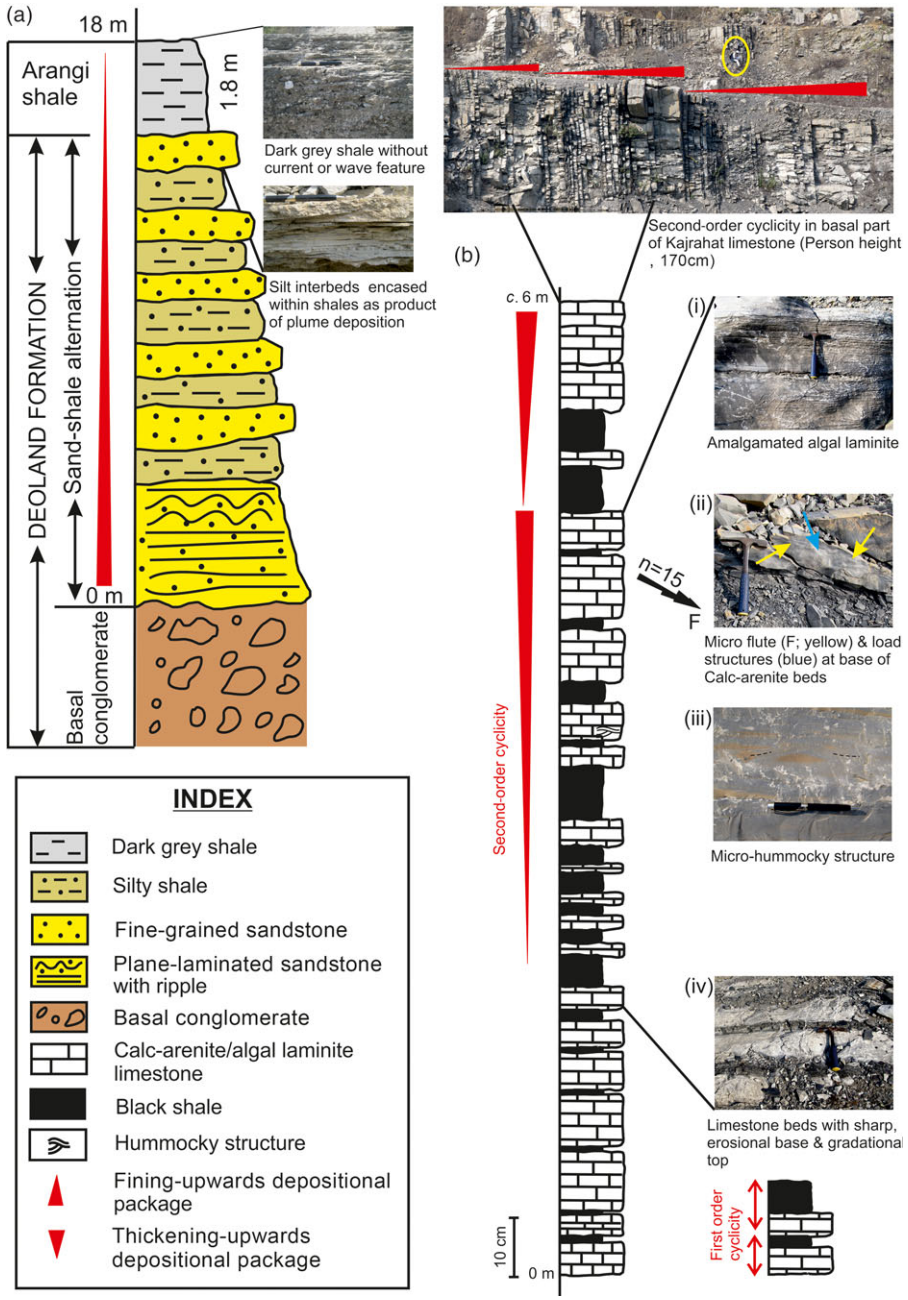

Fig. 2. (a) Litholog showing greenish-grey to dark-grey Arangi shale overlying Deoland Formation at Dalla, Uttar Pradesh. Note the fining-upwards stacking character. (b) Cyclic limestone – black shale alternation at the basal part of the Kajrahat limestone, illustrating the superimposition of depositional cyclicities. Field photographs showing (i) the algal micro-laminite; (ii) micro flutes and load structures; (iii) micro hummocks; and (iv) limestone beds with sharp erosional base and gradational top. Note the NW-wards palaeoflow direction of the micro flutes (hammer and pen length, 29 and 13.5 cm).

from a distal delta during high-energy events such as a storm (Fig. 2a; PP Chakraborty, unpub. PhD thesis, University of Jadavpur, 1996; Chakraborty & Sarkar, 2005). The supply of such plume materials offshore from a distal delta is reported from both modern (Okada & Ohta, 1993) and ancient geological records (Chakraborty & Bose, 1992; Sarkar *et al.* 2002*a*; Chakraborty *et al.* 2009; Sarkar *et al.* 2009).

From undoubted signatures of storm-induced flow within calcarenite limestone interbeds and their alternation with pyrite-bearing shale, it is inferred that the carbonate tempestites emplaced onto distal shelf beyond the oxygen minimum zone. Also, the calcarenite–shale alternation, with a stochastic, quasi-periodic bed thickness distribution of calcarenite beds, is interpreted as the signature of first-order depositional cyclicity within the Kajrahat shale. Crinkly algal micro-laminated bedded limestones are identified as the products of stratiform, benthic microbial mat growth predominantly within shallow water, possibly in an intertidal to peritidal domain (Grotzinger, 1989; Pratt *et al.* 1992; Sarkar & Bose, 1992; Sarkar *et al.* 1996). In these environments, laminites commonly record a combination of precipitation of fine-grained carbonate with benthic microbial mats and a trapping of detrital sediment (Grotzinger, 1986; Hamon & Merzeraud, 2008). The repeated gradual transition between distal shelf facies and shallow-water algal laminite bed-defining metre-thick cycles

https://doi.org/10.1017/S0016756820001168 Published online by Cambridge University Press

(Fig. 2b) possibly signify prograding depositional cycles of second order, developed during the process of distal to proximal shelf transition on Kajrahat carbonate platform (cf. Grotzinger, 1989).

3.b. Koldaha shale

The Koldaha shale occurs as the lower member of the Kheinjua Formation within the lower Vindhyan Group (Fig. 1b), and ranges in thickness from 350 to 600 m (Gupta *et al.* 2003). As a variegated shale unit, the Koldaha shale gradationally overlies the Porcellanite Formation, comprising dark-grey to greenish-grey splintery shale with sand and/or silt interbeds, and conformably passes into the overlying Churhat sandstone (Bose *et al.* 2001; Samanta *et al.* 2016). Rasmussen *et al.* (2002) constrained the age of Koldaha sediments as 1.60–1.63 Ga using U–Pb SHRIMP of zircon grains obtained from a tuffaceous interbed within this shale interval (Fig. 1b). Apart from recurrent punctuations caused by metre-thick coarse arenaceous intervals, the Koldaha shale succession registers repeated alternation of shale beds with storm-driven sandstone interbeds in widely varying volumetric proportion.

3.b.1. Argillaceous intervals

Three different types of shale units, classified on the basis of shale: sandstone ratio and thickness as well as the internal character of sandstone interbeds, define a major part of the Koldaha sedimentation history. The first interval (KDSH A; Fig. 3a(i), (ii)) is characterized by dark-grey to greenish-grey shale, often splintery with rare thin (< 2 cm) silt interbed(s) (average shale:sandstone ratio = 4.88). The bases of the silt units are dominantly planar, while the tops are locally undulated with small wave ripples. Wrinkle structures (amplitude < 1 mm; Fig. 3a(ii)) with widely varying relief, geometry and lateral continuity are noted on the bedding planes of silt interbeds. On close inspection, the shales reveal light- and dark-grey intertwined stripes showing growth of microbial mat, preserved in the absence of bioturbation (cf. Schieber, 1998; Chakraborty & Sarkar, 2005). In the absence of any sand interbed or any kind of wave- or current-related feature, this argillaceous interval suggests deposition in a prodeltaic outer-shelf setting near storm wave base (Banerjee, 2000; Bose *et al.* 2001; Samanta *et al.* 2016). The presence of wrinkle structures on bedding planes is probably due to gentle wave agitation on microbially mediated cohesive fine sand and/or silt surfaces during storm events (cf. Banerjee & Jeevankumar, 2005).

The second interval (KDSH B; average shale:sandstone ratio = 2.95) is marked by faintly laminated or massive grey, silty shale interrupted by centimetre-thick sheet sandstone beds with rare current ripples (average wavelength = 10 cm, amplitude = 2.2 cm; Fig. 3b). The sandstone beds are either massive or weakly graded with mudstone intraclasts near the base. Bases of these beds are carved with various sole structures such as flute, brush and tool marks, and internally these beds often show the presence of truncated T_{abe} or T_{abce} successions of Bouma (1962; Fig. 3b(iii)). Soft sediment deformation (SSD) structures, namely convolute lamination, flame and load structures (Fig. 3b(iv)), are common within these beds. Parallel-laminated, fine-grained sandstone grades to wavy-bedded silty argillite mimicking micro-hummock geometry (Fig. 3b(v)), with average wavelength 8 cm and amplitude 2 cm.

The sandstone interbeds with truncated 'Bouma' subdivisions are attributed to turbidite deposition from light-density flows or buoyant plumes in a mud-depositing environment. Such low-density flows in an otherwise very-low-energy environment can be generated by slope instability, storm-wave liquefaction of upslope fine-grained sediments (cf. Nelson, 1982), or dense fluvial bedloads that form turbid underflows on the seafloor (Boggs, 2006; Bera *et al.* 2008). The thin, laterally extensive nature of interbeds without any amalgamation and relatively low volume of sand are suggestive of a distal depositional setting. A base-of-slope setting seems plausible in view of the frequent occurrence of soft sediment deformation features (cf. Postma & Drinia, 1993; Chakraborty *et al.* 1998). The occasional sharp-based, fining-upwards sandstone interbeds recording upwards gradation from parallel lamination to hummocky cross-stratification are the result of gradually waning storm-induced traction currents, that is, late-stage storm-current activity below fair-weather wave base (Swift *et al.* 1987). Argillite drapes represent settling of fines, suspended during storm activity or under normal conditions (Chandler, 1984).

Greenish, mauve to red-coloured wavy-bedded shale represents the third argillaceous interval (KDSH C) with interbeds of thin siltstone (< 8 cm) and fine-grained sandstone (maximum recorded thickness, *c.* 20 cm; Fig. 3c); the volumetric ratio of sandstone to shale varies widely between 23 and 52%. The sandstone interbeds have sharp, erosional bases and gradational tops with parallel- to wavy-parallel lamination grading upwards into ripple cross-lamination. These beds either grade upwards into mudstone or are capped by wave or combined flow ripples with nearly straight crests, locally bifurcated and unidirectionally oriented foresets. Thicker sandstone interbeds are undulatory with pinch-and-swell bed geometry (Fig. 3c(ix)), and internally display small-scale hummocky cross-stratification with average wavelength and amplitude 22 cm and 8.5 cm, respectively (Fig. 3c(vii)). The soles of these sandstone beds bear swarms of brush marks or flute casts with NW–SE-trending symmetric and asymmetric gutters (Fig. 3c(vi), (viii)).

This shale unit is inferred to be a product of a storm-dominated inner to distal shelf, often extending up to storm wave base. Hummock-bearing sandstone interbeds with sharp, erosional bases and internal grading giving way upwards into combined flow-rippled bed tops indicate episodic storm deposition of sand in a normally mud-depositing environment, and suggest a high-energy gradient on the shelf (Dott & Bourgeois, 1982; Duke, 1985; Bose *et al.* 1988; Chakraborty & Bose, 1992; Banerjee, 2000). The intervening shale represents hemipelagic sedimentation during post-storm or fair-weather conditions, with a shallowing-upwards depositional pattern.

3.b.2. Arenaceous intervals

The Koldaha shale is interrupted by two major arenaceous intervals: (1) polymictic conglomerates with pebbly feldspathic poorly sorted sandstone (KDSH D); and (2) multi-storeyed, poorly sorted quartzo-feldspathic sandstone (KDSH E; Fig. 4a, b). The latter (KDSH D) consists of polymictic conglomerate of thickness *c.* 3 m (maximum clast size, *c.* 55 cm), successively overlain with pebbly, granular sandstone and coarse-grained granular sandstone. Conglomerates have non-erosive lower contacts and occasionally show normal concentration grading with the presence of pebbly and bouldery, angular or tabular clasts (size range, 0.5–55 cm) of shale, siltstone and porcellanite set in coarse, granular sandy matrix, indicating its matrix-supported character. The bed sets of conglomerates change inclination with change in bed dip from 2° (topset) to 30° (foreset) in an easterly direction (Fig. 4a(i)). Clasts are usually oriented with their long axes subparallel to the dip of the foreset beds. The maximum extent and height of the foreset was recorded as 12.5 m (in an E–W-aligned transect) and *c.* 2.5 m, respectively. Large-scale slump structures

https://doi.org/10.1017/S0016756820001168 Published online by Cambridge University Press

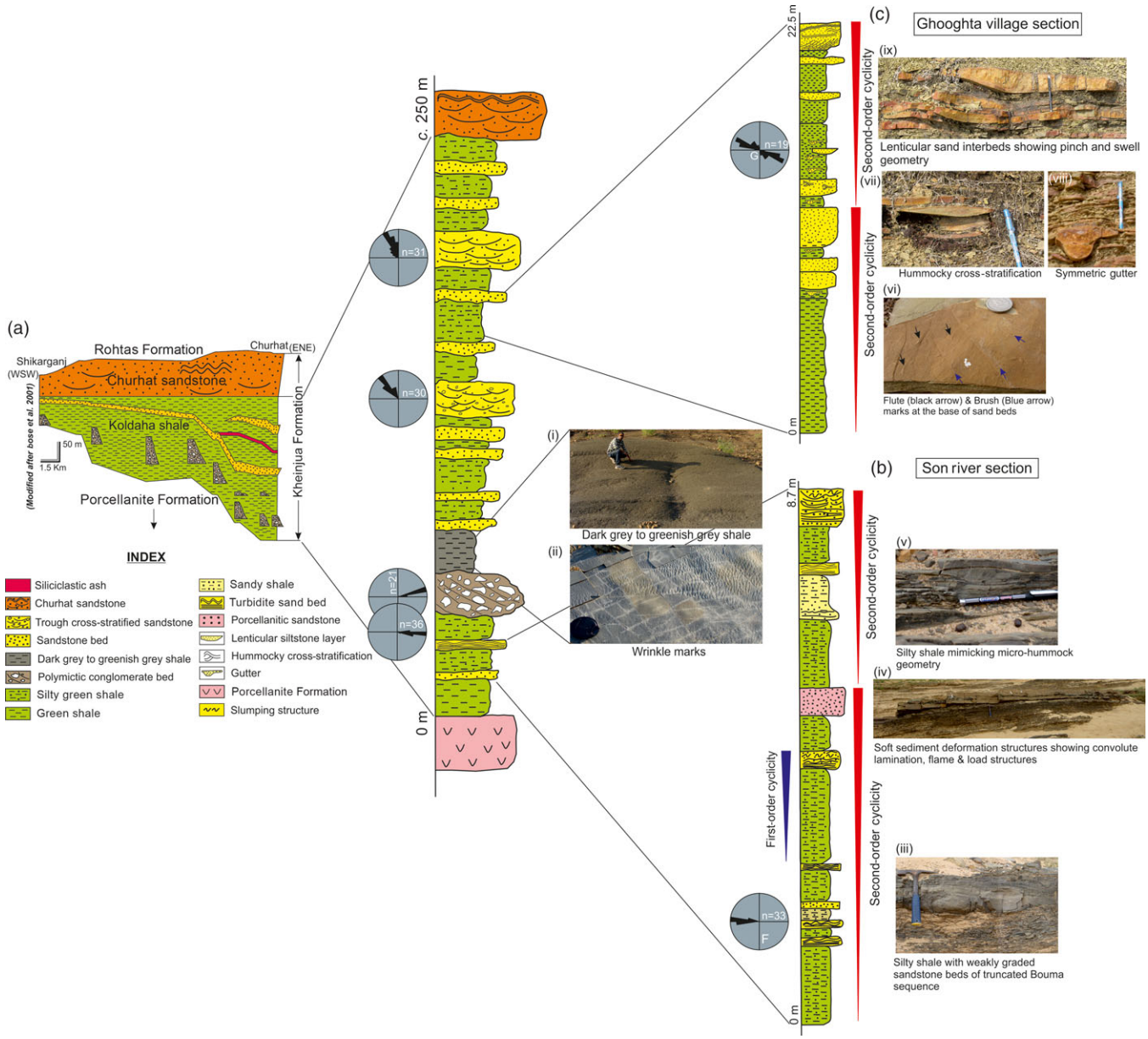

Fig. 3. (a) Correlative composite litholog of Koldaha shale between Shikarganj and Churhat consisting of (i) dark-grey to greenish-grey shale (KDSH A) with (ii) wrinkle marks on its bedding surface. Note wedging of arenaceous intervals towards both east and west. Also note the opposing (E- and W-wards) palaeocurrent from coarse arenaceous intervals present at different stratigraphic levels of Koldaha shale succession. (b) Composite and (c) detailed litholog of Koldaha shale from Son River and Ghooghta village sections. Note the presence of silty shale with weakly graded sandstone beds (KDSH B) of truncated Bouma sequence with (iii, iv) soft sediment deformation structures and (v) micro-hummocks in Son River section, and mauve- to red-coloured wavy bedded shale (KDSH C) with (vi) flute and brush marks, (vii) hummocks, (viii) symmetric gutters and (ix) sandstone interbeds with pinch and swell geometry in Ghooghta village section. Also note the W-wards palaeoflow of flutes (F) and NW–SE trend of gutters (hammer and pen length, 29 and 13.5 cm; person height, 175 cm; coin and cap diameter, 2.2 and 5 cm).

(average width, *c.* 60 cm; Fig. 4a(i)) are noted at the transition between the topset and the foreset strata. The pebbly granular sandstone and coarse-grained granular sandstones are planar to trough cross-stratified with average set and co-set thickness of 10 cm and 35 cm, respectively. Pebbles are often found strewn along the trough cross-strata with an E-wards palaeoflow direction (Fig. 4a).

Matrix-supported conglomerates with chaotic pebble- to boulder-sized clasts and non-erosional bases bear indication of deposition from high-density mass flows (Lowe, 1982; Vallance, 2000; Mulder & Alexander, 2001). The local presence of normal concentration grading, particularly at the basal parts of foreset strata, indicates deposition from subaqueous debris flows (Nemec & Steel, 1984; Pivnik, 1990). The crude horizontal-bedded coarse-grained sandstones that alternate with some of these debris-flow products may represent high-density turbidity flows (similar to the 'gravitational winnowing' of Postma, 1984) or coarse tails that follow behind debris flows. The overlying planar and trough cross-stratified pebbly and/or granular and poorly sorted granular sandstones are interpreted as the products of fluvial deposition. Overall, this conglomeratic unit is interpreted as the product of a tectonically triggered localized fan delta with suggestive Gilbert-type geometry. The very-coarse-grained character with the presence of angular, pebbly and boulder clasts derived from underlying strata (shale, porcellanite, etc.), the small aerial extent,

https://doi.org/10.1017/S0016756820001168 Published online by Cambridge University Press

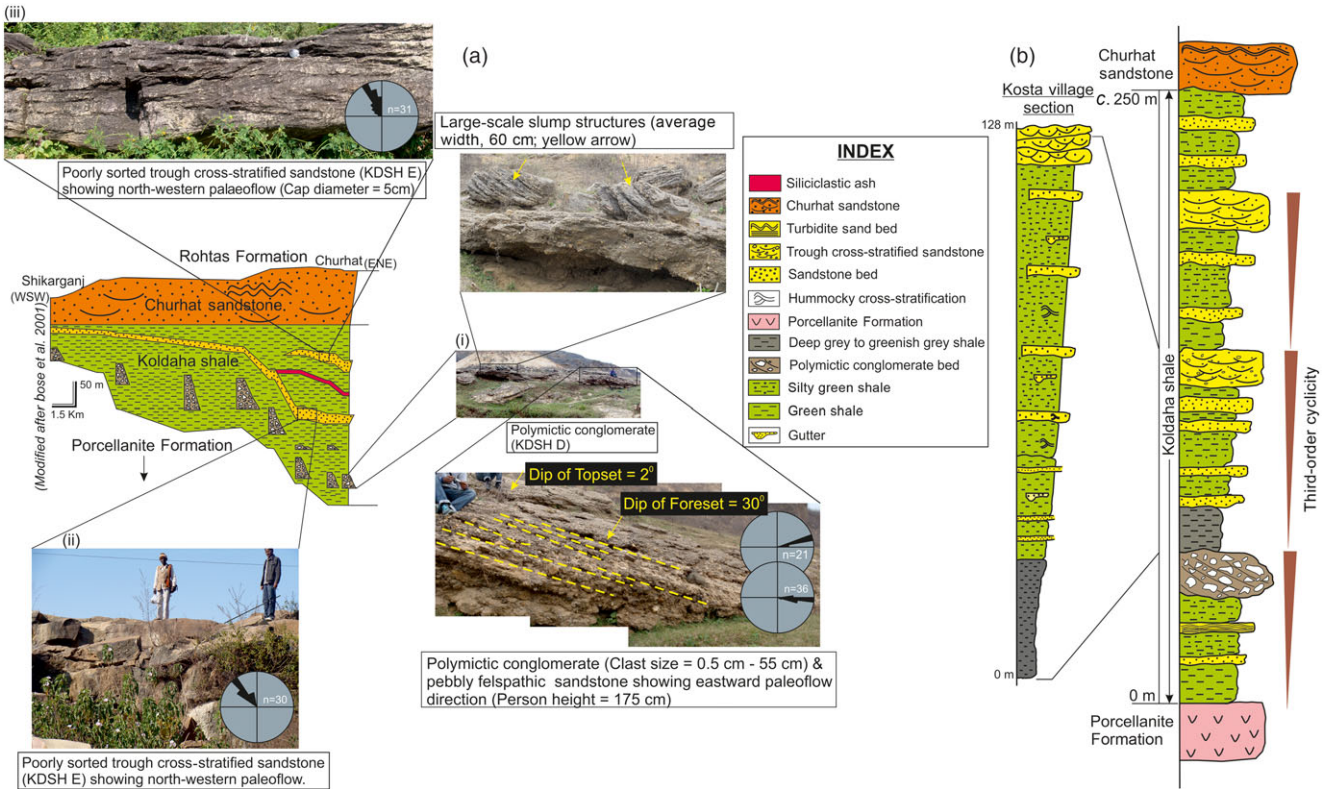

Fig. 4. (a) Relative stratigraphic position of coarse arenaceous intervals (fan delta (KDSH D) and fluvial origin (KDSH E)) in Koldaha shale. Note (i) the very large cross-stratification and slump structures in polymictic conglomerate (KDSH D) and (ii, iii) the trough cross-stratification in poorly sorted fluvial sandstone (KDSH E). (b) A composite litholog of Koldaha shale showing third-order tectonic and/or eustatic cycles bounded by coarse arenaceous units. Note the typical progradational stacking motif within individual third-order cycles recorded in the Kosta village section.

the wedging out of the entire unit in a downcurrent (E-wards) direction over a lateral width of *c.* 18 km with a decline in clast size, and the presence of structures indicating basinal instability (slumps, convolutes, etc.) all indicate the possibly fault-related tectonics-triggered supply of these fan delta sediments onto the shelf from a source in the west. While near-horizontal alluvial strata sets recording E-directed palaeoflow constitute the topset for this delta, the inclined strata sets composed of debris-flow products represent its foreset part. The signatures of slope instability and sediment failure within mass flows at the topset–foreset transition are well corroborated by the occurrence of convolutes, slump structures and small-scale faults. The argillaceous interval KDSH B (grey silty shale), which immediately underlies this conglomerate and/or granular sandstone package and hosts sandstone interbeds of low-density turbidite origin, represents the prodeltaic part of the inferred delta.

The other arenaceous interval (KDSH E) is characterized by the metre-thick multi-storeyed, poorly sorted quartzo-feldspathic sandstone present at two stratigraphic levels within the Koldaha shale succession (Fig. 4a(ii), (iii)). Each sandstone package displays a thickening-upwards stacking motif (Fig. 4b), where upwards coarsening of grain size culminates with the occurrence of granular lag at the tops of both the units (Bose *et al.* 1997; Banerjee & Jeevankumar, 2003). These sandstone units show tabular, fining-upwards cycles with multi-storeyed trough cross-stratifications (set and co-set thickness of *c.* 8 cm and *c.* 25 cm, respectively) with WNW-directed palaeoflow (Fig. 4a(ii), (iii)). Bose *et al.* (1997) reported rain prints, rain-impact ripples, desiccation marks, adhesion ripples and translatent strata from these sandstone packages, and also documented W-directed wedging of both units.

Poor sorting, tabular bed geometry, profusely present trough cross-stratifications displaying a unimodal palaeocurrent and fining-upwards depositional motif all indicate the fluvial origin of these sandstone units (Jones *et al.* 2006; Long, 2011; Chakraborty *et al.* 2012). The downcurrent wedging character for both sandstone packages in tandem with the first arenaceous interval indicate their supply from some localized slope with a much lower gradient compared to that of KDSH D. However, unlike KDSH D that wedges out towards the east, these sandstone packages wedge out towards the west. The W-directed palaeocurrent present within the sandstone packages suggests supply of these packages from a source in the east at times of intermittent relative fall in sea level. Sea-level fall and the emergence of the Koldaha shelf is attested by the occurrence of desiccation marks and aeolian features.

3.b.3. Depositional cyclicity

The argillaceous and arenaceous intervals of the Koldaha shale together constitute three different orders of cyclicity.

3.b.3.a. First-order cyclicity. This order of cyclicity represents the basic building block of the shale succession, in which basinal shale alternates with individual storm- or sediment-gravity-flow-deposited sandstones (average cycle thickness, 30–200 cm; Fig. 3). Considering the origin of sandstone interbeds as products of meteorological storms and shales as products of *in situ*

https://doi.org/10.1017/S0016756820001168 Published online by Cambridge University Press

sedimentation, this cyclicity is identified as a climate-driven event, depicting alternations between fair weather and high-magnitude storm-weather events. However, the sheet sandstones within KDSH B are interpreted as products of delta-fed mass flows in a prodeltaic set-up. The climate and tectonics individually or in combination can guide discharge variation in a fan delta (Nelson, 1982; Nemec & Steel, 1984; Jones *et al.* 2006). The sedimentation dynamics within a delta, namely channel switching, can also control the recurrence interval and volume of clastic supply in a prodelta setting. However, considering the omnipresent slump structures, convolutes and small-scale extensional structures within the sandstone interbeds of KDSH B (Fig. 3b), it is presumed that the supply of turbidites in the Koldaha prodelta setting is triggered mostly by tectonic forcing.

3.b.3.b. Second-order cyclicity. These cycles are of thickness 2–20 m and represented either by thickening- or thinning-upwards trends in sandstone interbed thickness (Fig. 3b, c). As well as an increase in the sandstone bed thickness, an individual thickening-upwards cycle is characterized by a transition from a dark-grey, silt-free shale to reddish silty shale and an increase in lenticularity of sandstone interbeds up-cycle. In contrast, the thinning-upwards cycles display a decrease in the sandstone:shale ratio and an increase in the dominance of dark-grey shale upwards. While dark-grey to black shale of distal shelf origin (KDSH A) marks the top of the thinning-upwards cycles, the heterolithic sandstone-red silty shale of proximal shelf origin (KDSH C) marks the top of the thickening-upwards cycles. However, storm bed thickness changes erratically between these orders of cycles, indicating a fluctuating sand depositional budget. Storm intensity and frequency, and its angle of direction with the shoreline and shelf gradient, individually or in combination, possibly controlled the budget (Myrow & Southard, 1996; S Banerjee, unpub. PhD thesis, University Jadavpur, 1997). These thickening- and thinning-upwards cycles are progradational or retrogradational in character. While gradual, progressively shallowing progradational cycles dominate the Koldaha succession, the thinning-upwards retrogradational cycles are rare, abrupt and often marked by disproportionate thicknesses of distal-shelf sand-free dark-grey to green shale. The fan delta association (KDSH D) is encased within one such fining-upwards retrogradational cycle, whereas the other two fluvial sandstone units (KDSH E) represent the tops of thickening-upwards progradational cycles (Fig. 4a). The occurrence of a fan delta showing slump folds, convolutes and other soft-sediment deformation structures, in association with a retrogradational cycle, indicates that tectonically triggered sudden subsidence prompted the deposition of disparately thick distal-shelf shale immediately above the fan delta.

3.b.3.c. Third-order cyclicity. Clusters of second-order cycles define third-order cycles, and resemble the third-order cycles of Vail's curve (Vail *et al.* 1977; Fig. 4b; average thickness, 60–130 m). Stratigraphically, thickening-, coarsening-upwards stratal packages and thinning- and fining-upwards packages are considered as products of alternate highstand and transgressive systems tracts (Van Wagoner *et al.* 1988; Banerjee, 2000). The disparately thick distal-shelf shale units (KDSH A) mark maximum bathymetry on the Koldaha shelf and are identified as products of maximum flooding. In contrast, stacks of progradational cycles with an increasing-upwards sandstone:shale ratio, topped by fluvial sandstones, mark the highstand depositional history on the Koldaha shelf. Although no time constraint is available, from the thickness of these cycles (tens of metres), Banerjee (2000) correlated these cycles with Vail's third-order curve (cf. Posamentier & Vail, 1988). Similar interpretations of cycles commonly related to glacio-eustasy are equally available (Cloeting, 1988; Miall, 2000), favouring tectonic forcing. The occurrence of palaeoseismic features at different stratigraphic levels of the Koldaha shale prompted us to correlate these cycles with tectonic forcing. Indeed, Bose *et al.* (1997) suggested the continuation of rifting within the Vindhyan Basin up to the time of Koldaha sedimentation.

3.c. Rampur shale

The approximately 85-m-thick Rampur shale is encased between the fine-grained marine siliciclastics of Kheinjua Formation (Sarkar *et al.* 2002*a*) below and the flaggy, bedded limestones of Rohtas Formation above (Fig. 5). Overall, the shale unit represents a fining-upwards succession, comprising well-sorted, fine-grained cross-stratified sandstone at the base, successively overlain by heterogeneous silty shale and siltstone and pyritiferous black shale, often interbedded with beds of siliceous tuff (Fig. 5). U–Pb zircon SHRIMP dating of interbedded tuff within the black shale reveals its deposition at *c.* 1599 ± 8 Ma (Rasmussen *et al.* 2002). The age of the Rohtas limestone overlying the Rampur shale is dated as 1601 ± 130 Ma by Ray *et al.* (2003) and 1599 ± 48 Ma by Sarangi *et al.* (2004) using Pb–Pb systematics. However, we consider the age of *c.* 1599 ± 8 Ma for Rampur shale more appropriate and convincing due to its lower error margin.

3.c.1. Sedimentation dynamics

The depositional history of the Rampur shale is described under three broad subdivisions. The basal lithounit is a buff-coloured, well-sorted, fine-grained sandstone with planar, quasi-planar to hummocky cross-stratification. NW–SE-oriented wave ripples occur as surface bedforms of sandstone beds (10–15 cm thick; Fig. 5a). Sarkar *et al.* (2002*a*) reported the presence of poorly sorted glauconite-rich sandstone pods with erosional bases and crude bi-convex laminae geometry within these quartz-rich sandstones.

The middle lithounit is characterized by greenish-grey shale of thickness *c.* 60 m with isolated fine-grained sandstone lenses that are normally graded, at times with the occurrence of mud clasts at their bases (Fig. 5b). These olive-green shales contain *c.* 1.1% TOC. Lenticular sand beds commonly show gutter casts, asymmetric in geometry. The average width and depth of gutters are measured as 32 cm and 12 cm, respectively, with their ratios ranging from 1.82 (base) to 3.38 (top) in a section of thickness *c.* 18 m recorded near Kudri village (Figs 1a, 5b(i)). Gutters are straight or slightly meandering and maintain a general NNW–SSE trend (Fig. 5b(i), (iii)). Internally, gutter fills are massive, plane-laminated or convex-up hummocky (Fig. 5b(ii), (iv)). Sole marks such as groove, prod and rare skip marks at the base of gutters show a parallel or near-parallel trend with that of the gutters (Bose *et al.* 2001; Sarkar *et al.* 2002*a*; AK Singh, unpub. PhD thesis, University of Delhi, 2015).

The greenish-grey shale grades upwards into finely laminated paper-thin black shale, completely devoid of any sand and/or silt interbed. The presence of dark black stringers, blebs and clots of organic matter, along with diagenetic pyrite, are characteristics of this shale (Fig. 5c). High TOC content of 2–5% corroborate this observation (Singh *et al.* 2018). The buff-coloured tuffaceous layers in alternation with black or grey shale often exhibit quenching cracks and normal grading.

https://doi.org/10.1017/S0016756820001168 Published online by Cambridge University Press

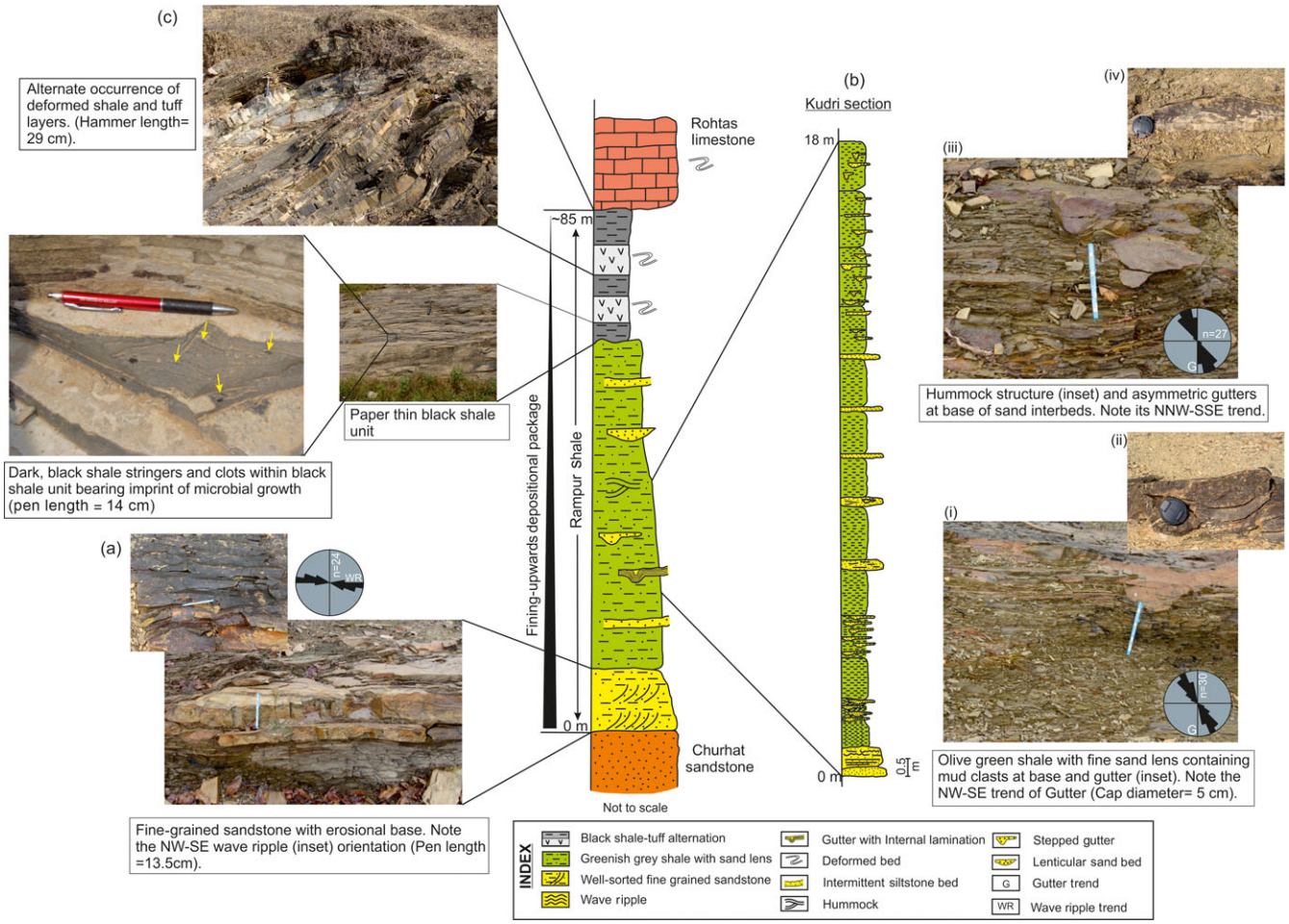

Fig. 5. Composite litholog of Rampur shale showing fining-upwards stacking motif, reconstructed from observations of the Kudri and Rampur nekin sections. Note the high-angle relationship of wave ripple and gutter trend. (a) Well-sorted fine-grained sandstone with wave ripples. (b) Detailed litholog and representative field photographs at Kudri section showing greenish-grey shale with (i) sand lens, (ii, iii) asymmetric gutters and (iv) hummock structures. (c) A slightly deformed black shale – tuff layer alternation at the top of Rampur shale, interpreted as the product of condensation.

3.c.2. Depositional environment

The Churhat sandstone of the Kheinjua Formation that underlies the Rampur shale comprises fine-grained marine siliciclastics (Bose *et al.* 1997) and is modelled as a product of sea-level high-stand (Bose *et al.* 2001; Sarkar *et al.* 2002*a*; Samanta *et al.* 2016). The initiation of shelf sedimentation of the Rampur shale is considered as a signature of transgression in the basin and defined as the product of a transgressive systems tract (Bose *et al.* 2001). The lower part of the Rampur shale is indicative of sedimentation in the lower shoreface and/or inner shelf within storm wave base (Fig. 5a). The quasi-planar and hummocky cross-stratification indicate the storm-infested nature of the shelf (Arnott, 1993) with mud deposition from suspension during the waning stages of storms (Sarkar *et al.* 2002*a*; AK Singh, unpub. PhD thesis, University of Delhi, 2015; Fig. 5a).

Greenish-grey shale without any current or wave features, as well as the absence of any sub-aerial emergence features (e.g. desiccation cracks), are interpreted as the product of suspension settlement in a shelf setting beyond fair-weather wave base (Fig. 5b). The sandstone interbeds with hummocks, gutters and sole marks are formed during high-energy events such as storms (Myrow, 1992; Chakraborty, 1995; Sarkar *et al.* 2002*a*, *b*). Gutters with near-consistent trend are the products of strong basal shear generated in the course of early storm flow, in which dragged particles grazed the surface and generated groove marks paralleling the gutters. While gutters and grooves record long-term storm-flow direction, the prod marks at high angles to gutters and grooves register instantaneous peak velocity of storm waves (Chakraborty, 1995; Stow *et al.* 2001). The asymmetric nature of the gutters is a reflection of current influence and storm flow on the Rampur shelf being more of a combined flow character, rather than purely wave-dominated. The increase in width:depth ratio of gutters upsection is indicative of progressively deeper shelf bathymetry. It is inferred that with an increase in bathymetry and flow path, there was decline in storm energy and gutters lost incision power and spread sideways. An inner- to middle-shelf domain is inferred.

Black fissile shale devoid of sand or silt interbeds and wave and/or current features is an indication of its deposition in a distal/outer-shelf setting beyond storm wave base (Fig. 5c). Reducing anoxic conditions in the Rampur distal shelf is inferred by the occurrence of pyrite. Samanta *et al.* (2011) considered the blebs and clots of dark black stringers within these shales as imprints of microbial mat growth. A gradual increase in bathymetry through the Rampur shale depositional history is inferred. Important changes noted upwards through the succession include: (1) a decrease in the number and thickness of sand interbeds, and

https://doi.org/10.1017/S0016756820001168 Published online by Cambridge University Press

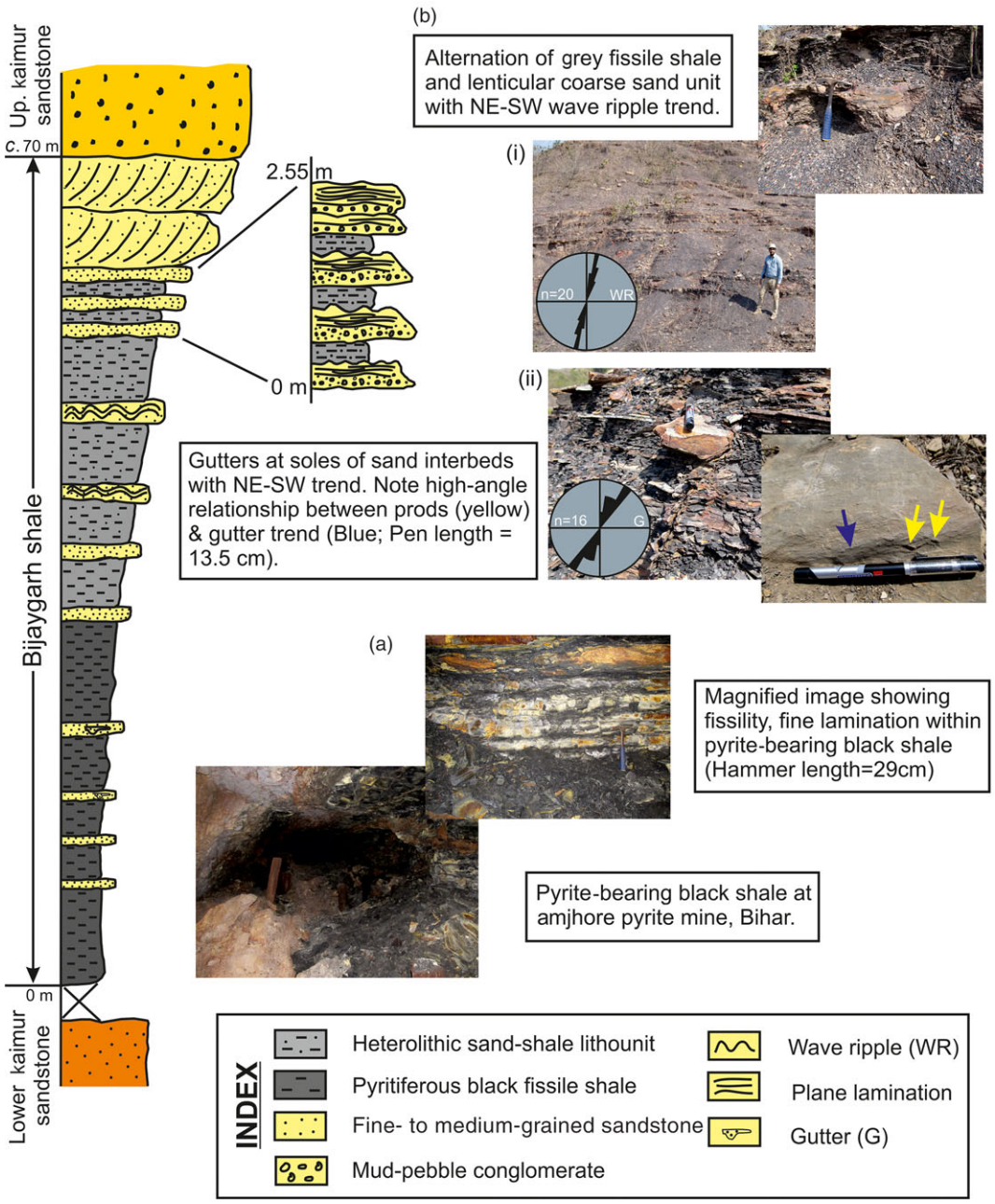

Fig. 6. Detailed litholog of Bijaygarh shale at Churk railway cutting section, showing progradational stacking motif with the occurrence of mud–pebble conglomerates in the topmost part. (a) Photograph showing pyritiferous black fissile shale at Amjhore, Bihar. (b) (i, ii) Representative photographs showing heterolithic sand–shale lithounit with gutters. Note the near-parallel orientation of wave ripple trend and gutter trend.

an increase in shale:sand ratio; (2) a change in the colour of shale from green- to dark-grey to black; (3) an increase in width:depth ratio of gutters; and (iv) the occurrence of volcaniclastic rocks at the topmost level of the Rampur shale immediately below the Rohtas limestone. The black pyritiferorus shale with interbeds of fine-grained volcaniclastic rocks at the top of this transgressive sequence is interpreted as the product of condensation (Kidwell, 1991; Bose *et al.* 2001). From consistent wave ripple crest orientation within both Khienjua Formation and the Rampur shale, an E–W-oriented palaeoshoreline is inferred for the Lower Vindhyan succession (Fig. 5a).

3.d. Bijaygarh shale

Bounded between silicified shale (Bose *et al.* 2001; Ramakrishnan & Vaidyanadhan, 2010) below and the scarp sandstone above (Chanda & Bhattacharyya, 1982), the Bijaygarh shale consists of a pyritiferous black shale and heterolithic sandstone-shale facies, and is best developed in the eastern and southeastern parts of the Son valley (Fig. 6a, b). Unlike Rewa and Bhander formations, the Kaimur Formation is intruded by lamproites with its surface expression in the Majhgawan region that was radiometrically dated (based mainly on Ar–Ar, Rb–Sr and K–Ar) as *c.* 1050 Ma (Crawford & Compston, 1969; Kumar *et al.* 1993; Gregory *et al.* 2006). A more precise age of *c.* 1210 ± 52 Ma for the Bijaygarh shale is assigned by Tripathy & Singh (2015) using an Re–Os geochronometer.

3.d.1. Sedimentation dynamics

Singh (1980) and Chakraborty (1995) documented the Bijaygarh shale succession as being of fining-upwards character with an increasing shale:sandstone ratio up the succession. However,

https://doi.org/10.1017/S0016756820001168 Published online by Cambridge University Press

detailed observation and measurement in the present study at Churk railway cutting section (Fig. 1) revealed a clear thickening and coarsening-upwards stacking motif. The black shale of offshore origin without any sand and/or silt interbed gives way upwards to the heterolithic sandstone–shale lithofacies, which suggests deposition within storm wave base (Fig. 6a). Pyrite, in the form of dissemination, massive or bedded (maximum 0.8 m thick at Amjhore, Bihar), has been reported from this shale with framboidal and euhedral habit (Sarkar *et al.* 2010). Microcrystalline quartz is seen with pyrite grains in the form of a 'teeth-and-socket' structure (Sur *et al.* 2006; Sarkar *et al.* 2010). At places, black, wispy carbonaceous laminae are also found in alternation with pyrite laminae.

Alternation between greyish fissile shale and sharp-based lenticular sandstone constitutes the heterolithic subdivision (Fig. 6b). While shale interbeds are structure-less, fissile with laterally variable thickness, the fine-grained (0.1–0.23 mm in size) sandstone interbeds have a sharp base, sharp to gradational top, and are internally plane to hummocky cross-stratified. Although most hummocks assume isotropic geometry with clear centripetally dipping laminations (cf. Harms *et al.* 1975, 1982), asymmetric geometry can also be noticed in some cases, where laminations dip preferentially in one direction (cf. Duke *et al.* 1991; Chakraborty, 1995). The average wavelength and amplitude of hummocks are 1.63 m and 0.18 m, respectively. Most of these sandstone interbeds are floored by straight to sinuous gutter casts and sole marks (prod and groove marks) that are observed on the walls of gutters (Fig. 6b(i), (ii)). The trends of gutters and wave ripples are similar, with a broad NE–SW orientation (Fig. 6b(i), (ii)). However, prod marks occur at a high angle to the gutter trend (Fig. 6b(ii)). Intermittently, the shale–sandstone heterolithic unit is punctuated by lenticular mud–pebble conglomerate beds topped by wave ripples with a ripple index of > 8. The increase in thickness of these conglomerate units can be noticed up the Bijaygarh shale succession.

3.d.2. Depositional environment

The sedimentation in the Bijaygarh shale started in an anoxic deep offshore (distal shelf) setting, as is clearly evident from (1) its black colour; (2) the presence of pyrite; and (3) the absence of any significant sand and/or silt interbed or wave and/or current feature (Fig. 6a). The alternation between wispy carbonaceous and pyritiferous laminae is inferred as the product of microbial growth of cyanobacterial origin (Schieber, 1989, 1999; Sur *et al.* 2006; Sarkar *et al.* 2010). The teeth-and-socket intergrowth between pyrite and quartz is suggestive of an early diagenetic origin of pyrite, which is also endorsed by its framboidal growth (Sarkar *et al.* 2010). Chakraborty *et al.* (1996) related the occurrence of a felsic tuffaceous unit at the topmost part of the Bijaygarh shale over a large aerial extent to the intrabasinal volcanism associated with major regression in the basin.

From orientation and infilling characters of gutters and their mutual relationship with trends of bed-top wave ripples, the operation of geostrophic current is suggested on the Bijaygarh shale shelf, and both long-term unidirectional current and instantaneous wave action controlled the orientation and filling history of the gutters. We interpret this as a combined flow regime, whereby geostrophic current is superimposed by wave action (Fig. 6a, b). The increase in bed thickness, degree of bed amalgamation and grain size of the sandstone interbeds up the Bijaygarh shale succession support the progradational history of the Bijaygarh shale and transition from offshore distal shelf to inner shelf. This contention is also corroborated by the occurrence of mud–pebble conglomerate units in association with storm packages in the inner-shelf deposits, and their increasing thickness up the succession (Fig. 6a, b). The confinement of mud–pebble conglomerates to the upper part of the Bijaygarh shale succession confirms inner-shelf palaeogeography as the storm return flow is likely to be the strongest, able to rip up mud clasts from the muddy substratum. The abundance and recurrence of sandstone interbeds within the Bijaygarh shale package is possibly controlled by the frequency and intensity of meteorological events, that is, storms on the shelf. With continuing progradation, the shelf succession of the Bijaygarh shale gives way upwards to nearshore conditions (Fig. 6b).

3.e. Rewa shale

Rewa shale, an informal term coined by Chakraborty & Sarkar (2005) combining the earlier proposed Panna shale and Jhiri shale (Auden, 1933), forms the lower part of the Rewa Formation and comprises three units: the Asan sandstone sandwiched between the Panna shale below and the Jhiri shale above (Bose *et al.* 2001). The shale succession, best exposed at the Sohagighat section, is composed of shale and sandstone interbeds with wave and sole features representing a storm-dominated shelf succession (Fig. 7a). Previous studies (Chakraborty & Chaudhuri, 1990; Chakraborty *et al.* 1996; PP Chakraborty, unpub. PhD thesis, University of Jadavpur, 1996; Bose *et al.* 2001; Chakraborty & Sarkar, 2005; Chakraborty, 2006) described the shaly, shelfal succession of the Rewa shale as a deep-water succession punctuated by wedge-shaped sandstone and/or conglomerate bodies occurring at multiple stratigraphic levels. Chakraborty & Sarkar (2005) interpreted these wedge-shaped sandstone and/or conglomerate units as regressive wedges with varying depositional environment. In the absence of any radiometric age, the discovery of a *Chuaria–Tawuia* association from the Rewa shale allowed assignment of a broad age range of 700–1100 Ma for this shale succession (Rai *et al.* 1997).

3.e.1. Sedimentation dynamics

Sedimentation in the Rewa shale started with the deposition of greenish shale interbedded with hummocky cross-stratified sheet sandstone. Shale laminae are persistent and thin, whereas sandstones are fine-grained, relatively thick (2–8 cm) and internally hummocky cross-stratified with domal geometry (Fig. 7a, b; cf. Harms *et al.* 1975). Hummocks are commonly developed on sets of plane laminae without erosion (cf. Brenchley & Newall, 1982; active hummock of Bose & Chanda, 1986; Bose *et al.* 1988). The amplitude and wavelength of hummocks vary over the ranges 8–10 cm and 1–2 m, respectively.

The greenish shale grades upwards into greenish-black to black shale without any persistent sandstone interbed (Fig. 7a–c). An alternation between laterally persistent, relatively thick shale (average, 18 cm thick) and siltstone laminae (average, 0.8 cm) form the basic framework for this shale. Shale laminae are dark, intertwined and do not persist laterally for more than 6 cm, whereas siltstone laminae are internally massive and laterally persistent. The basic motif of shale–siltstone interlaminae is interrupted infrequently by laterally discontinuous, sharp-based and wave-ripple-topped, well-sorted, medium-grained sandstone layers, stacked in a thickening-upwards motif (Fig. 7c).

Both green and black shale, in turn, are overlain by reddish-brown shale interbedded with fine-grained rippled sandstones

https://doi.org/10.1017/S0016756820001168 Published online by Cambridge University Press

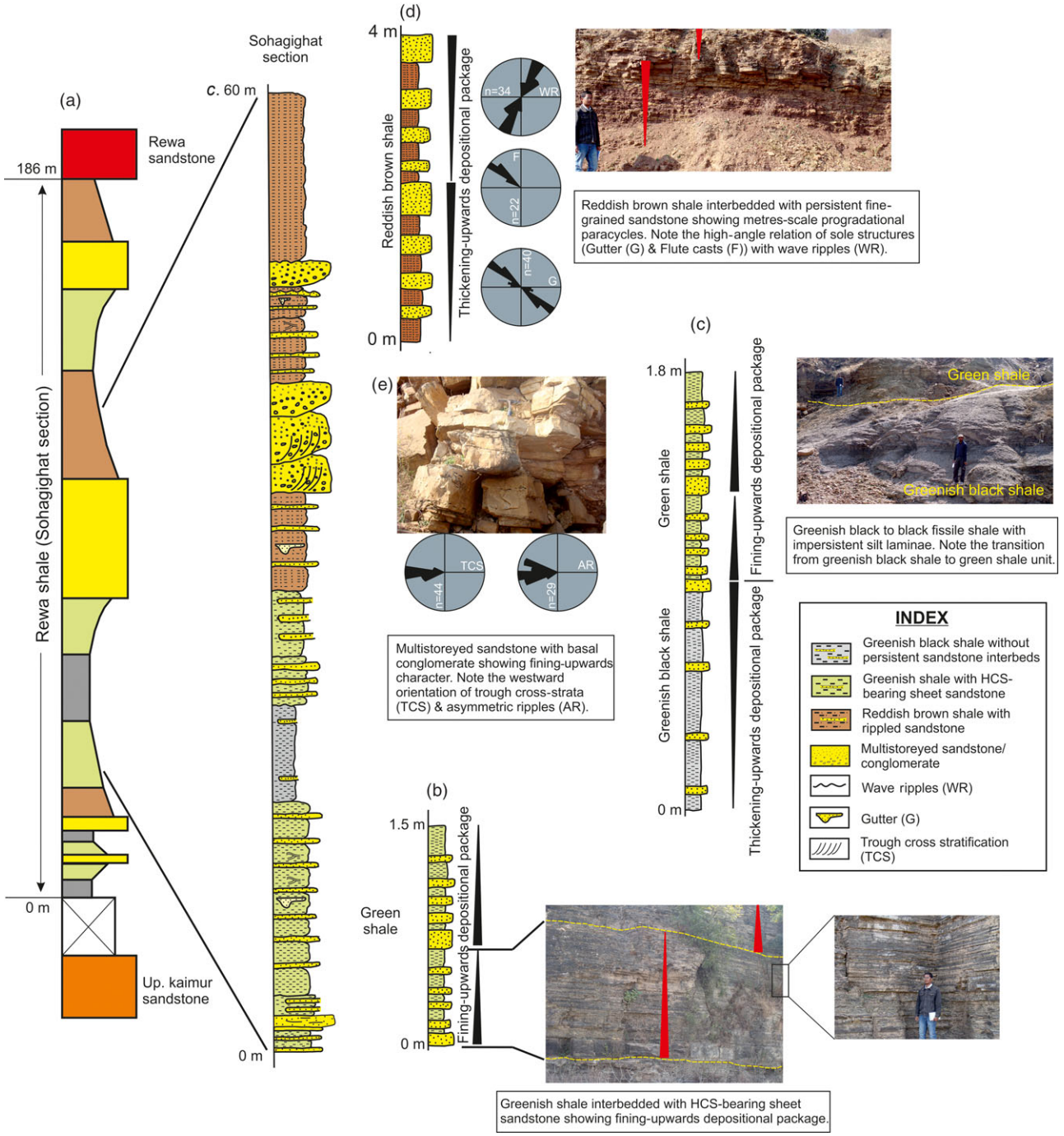

Fig. 7. (a) Composite litholog of the Rewa shale on the left (adapted from Chakraborty, 2006) and detailed measured litholog at Sohagighat section on the right. Lithologs representing (b) green shale lithounit with fining-upwards depositional package, (c) greenish-black fissile shale with impersistent silt laminae, (d) stacking pattern in reddish-brown shale lithounit showing thickening-upwards depositional package, and (e) spatially discontinuous metres-thick multi-storeyed sandstone lithounit at three different stratigraphic levels (person height, 175 cm). HCS – hummocky cross-stratification.

(2–40 cm thick) (Fig. 7a, d). The sandstone beds are sheet-like in geometry with internal laminations being sigmoidal, long-toed and of low angle in the downcurrent direction; in places, these give way into hummocks. Mud is mainly restricted to millimetre-thick veneers, which thicken within the ripple troughs. Internally, sandstone bodies comprise a basal lag of oxidized mud clasts followed up by plane lamination, co-sets of wave lamination including hummocky cross-stratification, and sandy ripples on top. Gutter and flute casts are frequently present at their soles (cf. Bose & Chaudhuri, 1990), and their orientation is at a high angle to the trend of wave ripples on bedding planes (Fig. 7d).

A spatially discontinuous metres-thick multi-storeyed coarse-grained siliciclastic package comprising conglomerate and coarse- to medium-grained sandstone punctuates the Rewa shale succession at the Sohagighat section (Fig. 7a, e). In a fining-upwards stacking motif, the siliciclastic lithopackage begins with a conglomerate unit at its base, and is successively overlain by multi-storeyed lenticular sandstone. Lenticular sandstones are characterized by a concave-up

https://doi.org/10.1017/S0016756820001168 Published online by Cambridge University Press

erosional base and conglomerate at their bases internally, followed by medium-grained sandstone. Sandstones become cleaner, finer and better-sorted moving up the storey, and the medium-grained sandstones are internally plane-laminated and trough cross-stratified. Symmetric ripples, with average wavelength and amplitude 4 cm and 0.6 cm, respectively, mantle these sandstones. Palaeocurrent measurements from ripples and trough cross-stratifications suggest W-directed bedform migration (Fig. 7e; Chakraborty & Sarkar, 2005; AK Singh, unpub. PhD thesis, University of Delhi, 2015).

3.e.2. Depositional environment

Greenish shale is more or less similar to black shale, except for the lower shale:sand ratio compared with black shale. It is therefore inferred that while black shale was deposited distally offshore below storm wave base, greenish shale represents its shallow counterpart in the more proximal part of the shelf above the storm wave base. The occurrence of small hummocky cross-stratifications (< 1 m) within sandstone interbeds of green shale clearly indicate the storm-infested character of proximal shelf (Bourgeois, 1980; Hunter & Clifton, 1982; Bose & Chaudhuri, 1990). A lack of evidence of reworking on top of inferred storm-generated beds indicates that deposition of these beds took place below fair-weather wave base, but within storm wave base (Bose *et al.* 1988).

The upwards transitions from green shale to both black and reddish-brown shale imply depositional environment of the green shale midway between the inner (red brown shale) and outer (black shale) shelf. The slow transgression and regression of sea level on the Rewa shelf was responsible for the retrogradational and progradational transitions (Fig. 7b–e).

All three types of shale units are free of emergence features except for some selective 2-m-thick intervals at every upwards transition from the greenish shale to reddish-brown shale. The emergence features include runzel marks, rain prints, rain-induced ripples and polygonal sand-filled cracks of possible desiccation origin, along with interference and superimposed ripples and salt pseudomorphs (PP Chakraborty, unpub. PhD thesis, University of Jadavpur, 1996; Chakraborty & Sarkar, 2005). The emergence features, particularly the mud cracks, may penetrate the topmost level of greenish shale immediately underlying the sharp green to reddish-brown shale transition, but more often remain confined to the basal zone of the overlying reddish-brown shale. Considering the inferred palaeogeographic setting of the different shale lithounits, the presence of emergence features at specific stratigraphic levels indicates multiple events of large-scale regression. In fact, the coarser terrigenous package that intervenes the Rewa shale succession at the Sohagighat section (inferred as regressive deposits; Chakraborty, 2006) coincides with one such sharp upwards transition from greenish to reddish-brown shale (Fig. 7c, d).

3.f. Sirbu shale

The Sirbu shale, bounded by Lower Bhander sandstone of coastal playa origin below and marginal marine Upper Bhander sandstone above, forms the youngest argillaceous succession in the Vindhyan sedimentation history (Chanda & Bhattacharyya, 1982; Bose & Chaudhuri, 1990; Bose *et al.* 1999; Sarkar *et al.* 2002*b*). From reports of putative occurrence of carbonaceous megafossils, cyanobacteria, acritarchs and Ediacara fauna in Sirbu shale and underlying Lakheri limestone, a broad age range of *c.* 650–1000 Ma (Neoproterozoic) is suggested for the Bhander Group (Kumar & Srivastava, 1997, 2003; De, 2003, 2006; Prasad, 2007; Srivastava, 2009). However, recent studies involving detrital zircon geochronology and palaeomagnetism from the Upper Bhander sandstone (Malone *et al.* 2008) and Pb–Pb isotope ages from the Lakheri limestone (Gopalan *et al.* 2013) allowed a strong suggestion for the *c.* 1000 Ma closure of Bhander sedimentation in general, and a marginally older age (> 1000 Ma) for the Sirbu shale in particular. Except for a few oolitic and stromatolitic carbonate beds occurring at its base, the Sirbu shale is represented by a monotonous shale succession until it is overlain by shallow-marine terrestrial sandstones of the Upper Bhander sandstone (Bose *et al.* 1999; Sarkar *et al.* 2002*b*; AK Singh, unpub. PhD thesis, University of Delhi, 2015).

3.f.1. Sedimentation dynamics and depositional environment

3.f.1.a. Carbonate intervals. Carbonates at the basal part of the Sirbu shale are represented by stromatolite–algal laminite and oolitic limestone (Fig. 8). Large cabbage-headed stromatolites (average column width and height, 26 cm and 9.1 cm; width:height ratio, 2.5–3.2) with domal, hemispheroidal geometry inflate upwards into algal laminite. Columns are symmetrically developed (column wall inclination, *c.* 30–40°C) with shallow columnar area, giving a cabbage-like shape (Fig. 8a). The sand-sized stromatolitic fragments and pyrite grains are found dispersed in shallow trough-shaped intercolumnar areas. In the tabular oolitic limestone (30 cm thick) unit, allochems including ooids, peloids and intraclasts are found floating within micritic and/or sparitic orthochemical groundmass (Fig. 8b).

The occurrence of concentric ooids with circular cross-sections, peloids and intraclasts is suggestive of ooid shoal development in a high-energy coastline. In contrast, stromatolites with cabbage-headed geometry, symmetrical growth of the column, high width:depth ratio, narrow intercolumn, laterally persistent laminae and dispersed pyrite grains all indicate low-energy, euxinic conditions, possibly at the back of a barrier (Sarkar *et al.* 1996; Chakraborty, 2004). Considering the shallow-water bathymetry, a peritidal depositional condition including an oolite shoal, lagoons and intertidal flats is postulated.

3.f.1.b. Terrigenous intervals. Above the carbonates, the Sirbu shale succession commences with greenish-black shale, characterized by repeated alternation between laterally persistent thick shale and thin siltstone laminae (sand:shale ratio, 0.02; Fig. 9a). Shale laminae are intertwined and wrinkled, forming dark shaly wisps, whereas lenticular siltstone laminae are internally massive, plane-laminated or cross-stratified without any wave features, channel-cut or emergence feature, and therefore suggest deposition beneath the storm wave base, in a calm and quiet distal offshore setting. The presence of intertwined dark shaly wisps indicates the role of microbial mats in deposition (Schieber, 1986, 1998; Sarkar *et al.* 2002*b*, 2005; Singh *et al.* 2013).

The greenish-black shale is overlain by green shale, often interbedded with tabular sandstone and higher sand:shale ratio (0.05; Fig. 9b). Internally, these sandstone interbeds show plane lamination and hummocky cross-stratification with amplitude and wavelength of 5–10 cm and 15–22 cm, respectively. Increased sand:shale ratio and hummocky cross-stratification suggests a storm-infested shoreward setting, in comparison to sand-free greenish-black shale that represents a distal offshore setting.

The green shale further grades upwards into grey shale, frequently interbedded with lenticular sand beds (Fig. 9c), with still

https://doi.org/10.1017/S0016756820001168 Published online by Cambridge University Press

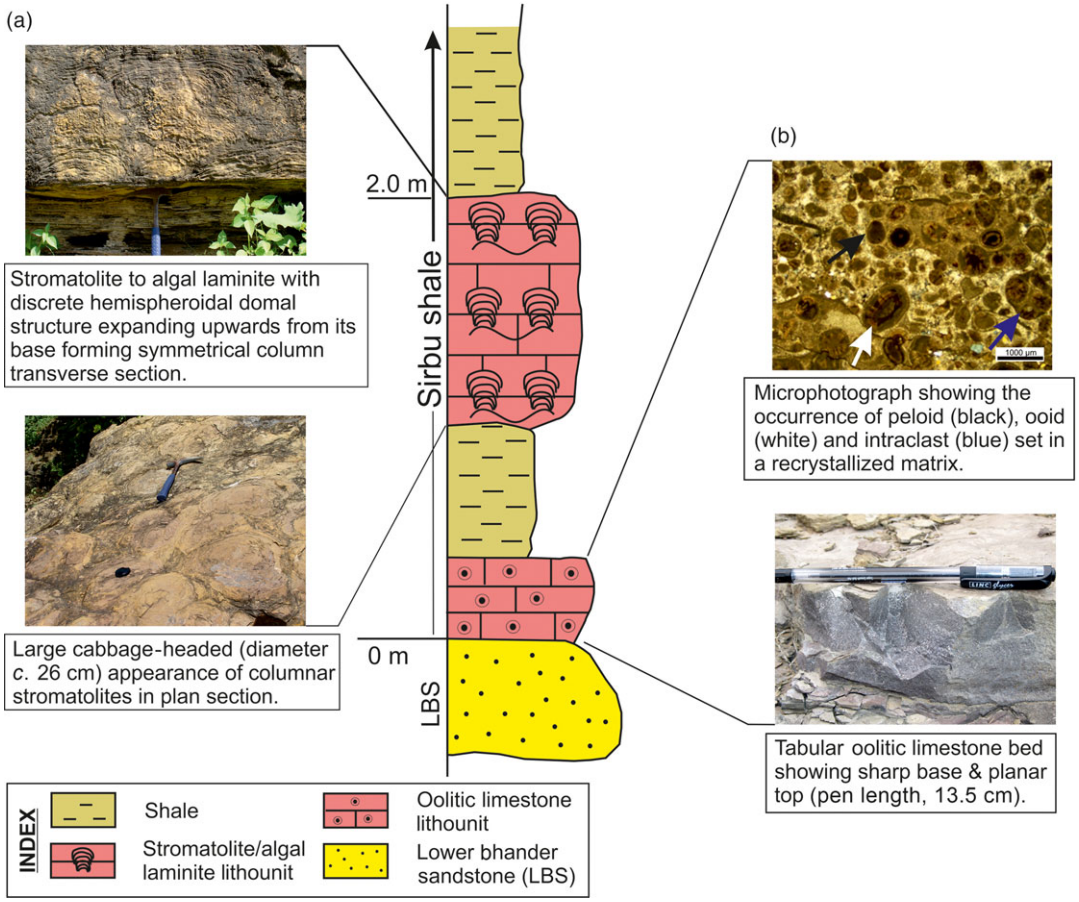

Fig. 8. Litholog showing (a) stromatolite–algal laminite and (b) tabular oolitic limestone from basal part of the Sirbu shale (hammer length, 29 cm).

higher sand:shale ratio (0.09). These lenticular sand beds occur with sharp base, gradational top, are internally normal graded with U-shaped gutters (width, 10 cm; depth, 2 cm) and wave ripples. Gutter and wave ripple trends have a high-angle relation to each other, whereas prod marks on the walls of gutters have a similar NW–SE trend to that of the gutters (Fig. 9c). A grey colour, relatively higher sand:shale ratio and the presence of gutters reveal deposition in mid-shelf at a depth shallower than that of the green and black shale. The orientation of gutters, prod marks and wave ripples suggests the operation of geostrophic flow on the Sirbu shelf, with shale interbeds as the products of suspension fallout and sandstone interbeds the product of high-energy flows.

The grey shale is gradually succeeded by reddish-brown silty shale, marked by the presence of fine-grained, laterally persistent, tabular sand beds (Fig. 9d) and the highest sand:shale ratio (0.42). Sand beds are massive, plane-laminated, convex-up or sigmoidal cross-laminated with sharp base and a gradational to sharp top with NE–SW-orientated symmetric ripples on bedding planes (Fig. 9d). The bases of these beds are marked by symmetric gutters. The reddish-brown colour, high sand:shale ratio and thick sandstone interbeds with wave ripples suggest an inner shelf – distal shoreface setting within the fair-weather wave base.

A sandstone unit of thickness *c.* 35 cm interrupts the Sirbu shale succession at its lower part, and is exposed around the Beehita area (Fig. 9e). The sandstone is tabular in geometry, fining-upwards in character and encased between greenish-black shale below and green shale above. No repetition of this unit is noticed in the Sirbu shale succession, which is of thickness *c.* 130 m. Internally, the fine-grained sandstone bed shows a patchy mud–pebble conglomerate unit overlain by a quasi-planar lamination, planar lamination and co-sets (average set thickness, *c.* 5 cm) of trough cross-stratification (Fig. 9e). An exceptionally well-preserved development of a microbial-mat-induced structure (MISS) is observed on the bed surface (Fig. 9e). Wave and current ripples (average wavelength and amplitude, 19 and 1.5 cm, respectively) of NW–SE-aligned ripple trend are also common on its bed surface (Fig. 9e). The sharp erosional base, normal size grading and the presence of structural sequence resembling the Bouma T_{abc} cycle point to a mass-flow event as a result of a tectonic or climatic perturbation (Kuehl *et al.* 1989; Shanmugam *et al.* 2000; Carvajal & Steel, 2006; Shanmugam, 2006). The prolific growth of bacterial mat indicates the otherwise starved condition of the basin where the mass flow became emplaced.

The carbonate package at the basal part of the Sirbu shale succession records the initiation of its deposition on the coastal playa of the Lower Bhander sandstone with the rise in relative sea level (Fig. 8). From the occurrence of a thin openwork conglomerate layer with early pore cement immediately above the stromatolites, Sarkar *et al.* (2002*b*) suggested the formation of the transgressive lag in high-energy conditions with the rapid rise in sea level on the Sirbu shelf, and therefore substantial transgression (cf. Smith & Lowe, 1991; Walker & Plint, 1992; Chakraborty & Paul, 2008). The rapid sea-level rise possibly pushed Sirbu shelf depth below the photic zone and forced the termination of carbonate production, as evident from the occurrence of greenish-black and green shale directly above the stromatolites (Figs 8, 9). However, the

https://doi.org/10.1017/S0016756820001168 Published online by Cambridge University Press

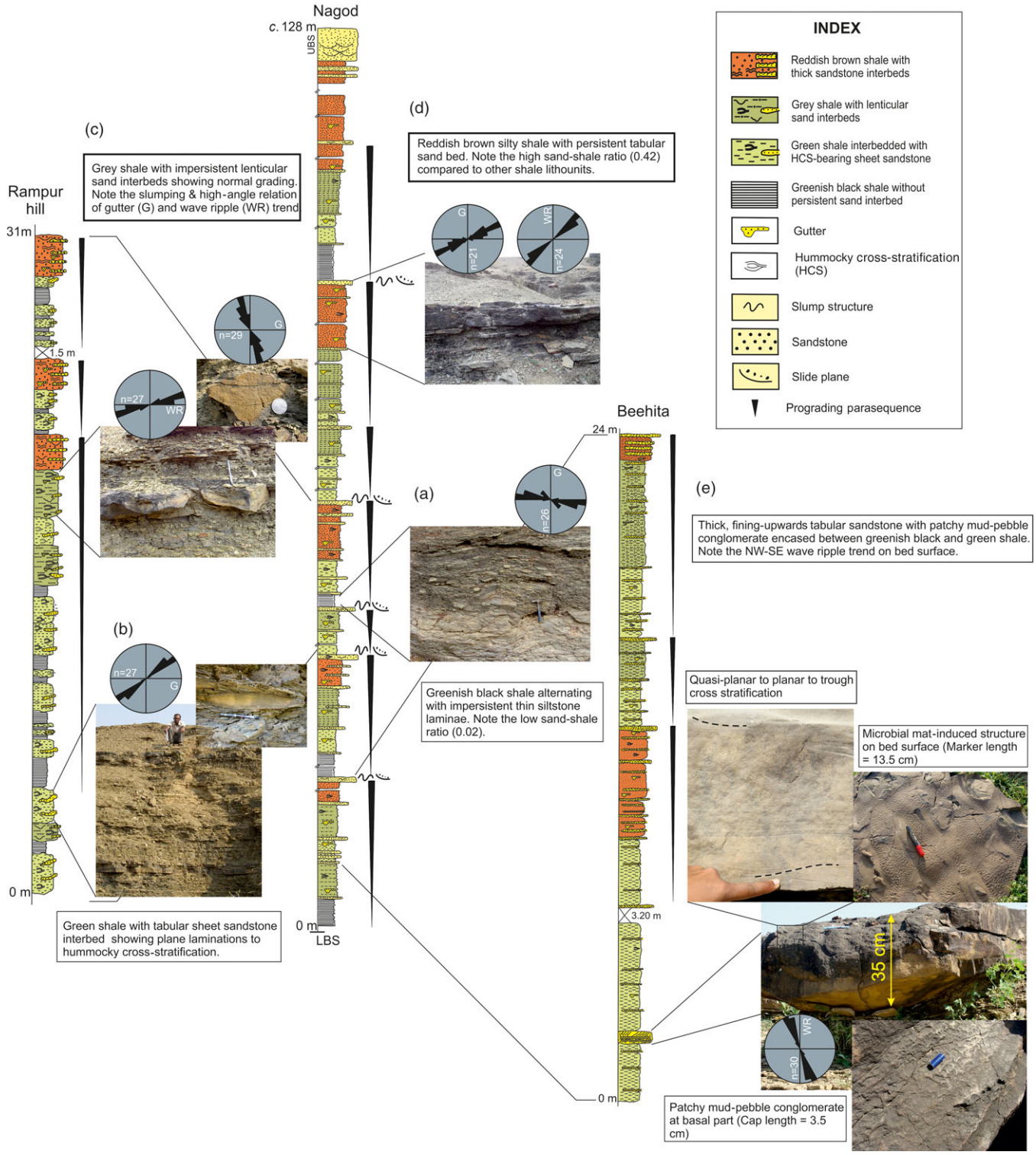

Fig. 9. Detailed litholog of the Sirbu shale from Nagod, Rampur hill and Beehita sections showing stacking of metres-thick progradational packages. Note the invariable occurrence of slump folds and slide planes at the topmost sandstone bed of each progradational package. (a) Greenish-black shale with thin siltstone laminae, (b) green shale interbedded with thick tabular sandstone, (c) grey shale with impersistent lenticular sand bed showing normal grading, (d) reddish-brown silty shale with laterally persistent tabular sandstone showing similar gutter and wave ripple trend, and (e) photographs showing characteristics of fining-upwards tabular sandstone unit at Beehita section, encased between greenish-black and green shale lithounit (hammer and pen length, 29 and 14 cm; person height, 165 cm; coin diameter, 2.6 cm); LBS – Lower Bhander sandstone, UBS – Upper Bhander sandstone.

https://doi.org/10.1017/S0016756820001168 Published online by Cambridge University Press

occurrence of grey and reddish-brown shale with relatively thick sand interbeds towards the top of the Sirbu shale succession suggests the shallowing and prograding character of the shelf in its transition to the Upper Bhander sandstone. The stacking of a number of metres-thick thickening-upwards (shoaling) hemicycles constitutes the overall progradational stacking motif. We identified these metres-thick hemicycles (2–20 m in thickness) as sets of higher-frequency sequences of lower hierarchical rank (cf. Zecchin & Catuneanu, 2013), and noticed the invariable presence of deformational structures such as slump fold, slump scar, slide plane etc. at the topmost sandstone interbed of each hemicycle (Fig. 9). Acknowledging the high degree of variability in the expression of sequence-stratigraphic units and their bounding surfaces, namely parasequence, small-scale cycle, etc. and the methodological confusions generated, Catuneanu *et al.* (2010) argued for uniformity in expression and suggested the use of the sequence concept for the classification of high-frequency cycles related to transgression and regression in shallow-water settings. Bose *et al.* (2001) and Sarkar *et al.* (2002*b*) surmised a stepped progradation for the Sirbu shale with each progradational cycle terminated by flooding caused by repeated basin-floor subsidence. A decline in the rate of subsidence and an increase in the rate of sediment flux possibly resulted in long-term progradation during the Sirbu shale depositional history.

4. Discussion

4.a. Controls on depositional dynamics

4.a.1. Operative processes, variabilities and controls on stratal stacking

The process-based sedimentological study of the Vindhyan shales clearly indicates their deposition in a marine realm with environmental settings ranging from distal shoreface to distal shelf beyond storm wave base (Singh, 1980; Chakraborty, 1995; Bose *et al.* 2001, 2015; Sarkar *et al.* 2002*a*, *b*; Fig. 10a–f). Like most documented Precambrian shelf deposits (Schieber, 1989; Jackson *et al.* 1990; Lindsey & Gaylord, 1992; Tirsgaard & Sønderholm, 1997; Eriksson *et al.* 1998; Sarkar *et al.* 2002*a*; Chakraborty & Sarkar, 2005), the Vindhyan shelf was also frequently infested by storms that led to the operation of both storm return flow and geostrophic flow. While signatures of storm return flow are observed from Rampur, Rewa and Sirbu shale successions (Figs 5a, b, 7d, 9c) as a result of the high-angle relationship between wave ripple and gutter trend within the storm deposits, unequivocal evidence for the operation of geostrophic current is documented from the Bijaygarh shale succession (Fig. 6b). The shelf gradient would definitely have played a major role in the character of storm-flow operation, and return flow would have been favoured in relatively higher-gradient shelves. Nonetheless, a strong energy gradient is recorded from the proximal to distal Vindhyan shelf as represented by a decrease in thickness, lenticularity and degree of amalgamation of storm deposits, which also helped in deciphering relative bathymetry of the shelf in otherwise fossil-poor conditions. The occurrence of hummocky cross-stratification, wave ripples and prod marks with reversing orientation are all evidence of an oscillatory component in the flow, whereas asymmetric gutters, flutes and wave and current ripples are evidence of the operation of a current component. However, we could not detect any systematic change in the nature of sole markings (gutter, flute, prod and brush marks) in storm products of different depth. The orientation of fair-weather wave ripples recorded from shale successions suggests that the Vindhyan shoreline trend varied from E–W-aligned to NE–SW-aligned, and remained persistent throughout its depositional history. Wherever the operation of geostrophic current is interpreted (e.g. Bijaygarh shale), the orientation of the sole features indicates that the seawards or W-wards down-welling flow was deflected and became shore-parallel. In addition to tempestites, the operation of the turbiditic flows on the Vindhyan shelf is also documented from the Koldaha and Sirbu shale successions, either in a prodeltaic setting (in the case of Koldaha) or as lone tectonically and/or climatically triggered sandy mass flow (in the case of the Sirbu shale) (Figs 3b, 9e). The frequent presence of deformational structures (convolute bedding, diapiric and loading structures) in such deposits attests to a relatively higher slope of depositional palaeosurface and high sedimentation rates.

Stratal stacking patterns of shale successions indicate depositional cyclicities of different orders as well as their varied forcing mechanisms. Developed in an overall transgressive (Arangi and Rampur shales) or regressive (Koldaha, Bijaygarh, Rewa and Sirbu shales) depositional motif, the shale units record imprints of different depositional controls that vary from event-scale to basin-scale. The most fundamental among these controls is the alternation between individual sand and/or silt bed and shale. If the identification of sandstone and/or siltstone interbeds within shale successions as products of meteorological storms is correct, then the alternation between fair-weather and extreme-weather products can be considered as first-order cyclicity. Working on stratigraphic records, Hamblin & Walker (1979) estimated storm recurrence interval on a shelf as 4033–12 000 years, which far exceeds the span of human life (Dott, 1996). Considering it as a skewed record, heavily biased towards major storm events, Banerjee (1996, 2000) argued for storm periodicity in relation to the Milankovitch climatic cycles. The next order of cycles, often metres to tens of metres in thickness, involves a number of beds and/or bed sets and is represented in the form of both a progradational (coarsening-upwards) or retrogradational (fining-upwards) stacking motif, and interpreted as high-frequency sequences following the recently accepted nomenclature of sequence stratigraphic units and their bounding surfaces (Catuneanu *et al.* 2010; Catuneanu, 2017). While those cycles of uniform character (e.g. progradational; Koldaha and Sirbu shales) stack together to build up the overall stacking fabric of shale formations (Figs 3, 4, 9), an alternation between cycles of two different characters, namely progradational and retrogradational, build up the stacking motif in some other shale formations (e.g. the Rewa shale) (Fig. 7). Undoubtedly, the balance between the rate of accommodation space generation (basinal tectonics and/or sea-level change) and the sand depositional budget (dependent on intensity, proximity or incidence angle of storm, as well as the advancement or recession of shoreline) controlled these cycles, which, in the absence of age data, could not be underpinned with any specific mechanism. Only in the Sirbu shale, where penecontemporaneous deformation structures (e.g. slump structures or slide planes) invariably occur at the topmost part of each progradational cycle, and the immediate superjacent cycle starts with deepest-water facies, could a tectonic origin for the cycles be advanced with certainty.

4.a.2. Coarse arenaceous intervals: fingerprints of tectonics and sea-level variations

With ongoing rifting in the basement leading to opening of the basin, there was deepening of the Arangi shelf. This led to the deposition of grey to black shales with intermittent feldspathic siltstone interbeds on the steeply dipping footwall, whereas

https://doi.org/10.1017/S0016756820001168 Published online by Cambridge University Press

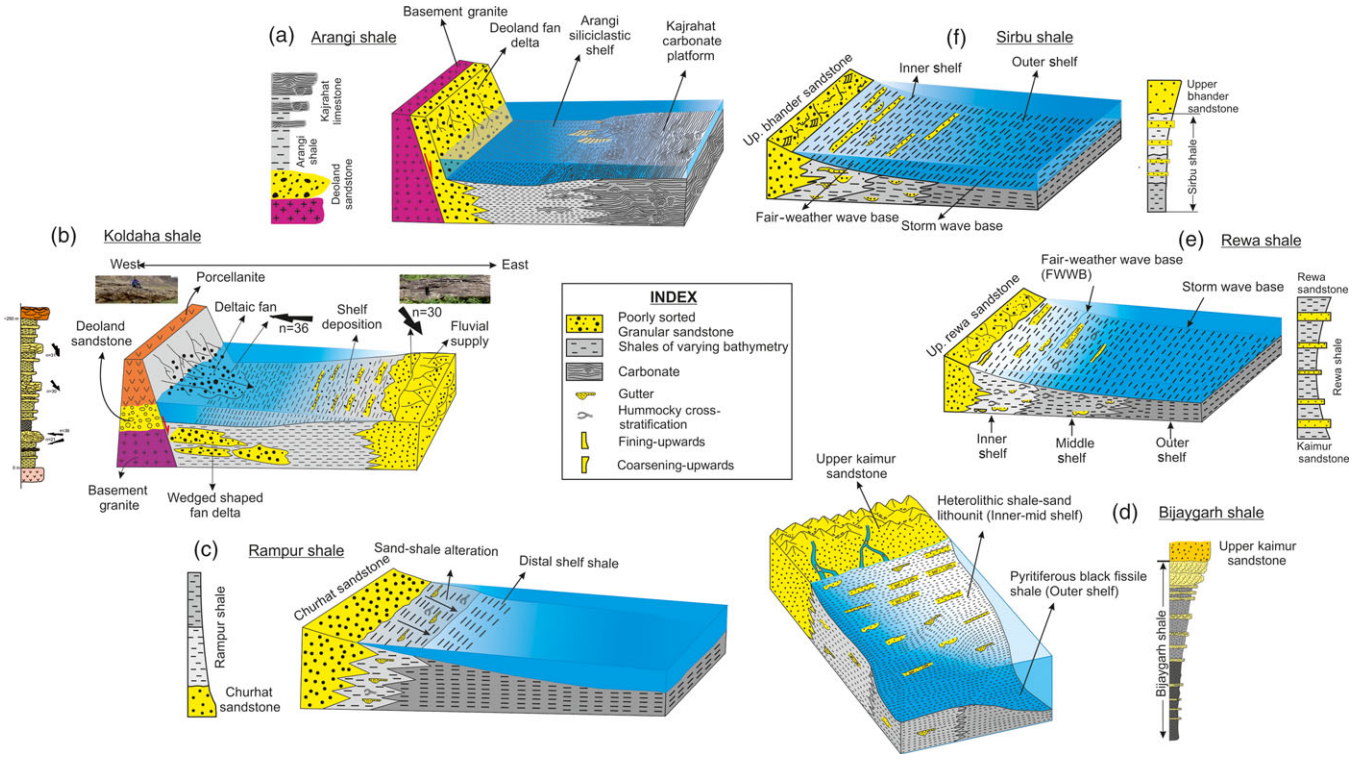

Fig. 10. Depositional models for (a) Arangi, (b) Koldaha, (c) Rampur, (d) Bijaygarh, (e) Rewa and (f) Sirbu shales. A half-graben model is proposed for both Arangi and Koldaha shales. While the hanging wall of the half-graben is represented by the Kajrahat Carbonate platform during the deposition of the Arangi shale, it was a fluvial system in the hanging wall during the deposition of the Koldaha shale. Note the oppositely oriented palaeocurrent for the fan and fluvial system in the Koldaha basin. Note also the termination of rift-stage sedimentation and the establishment of the shelf system with a well-developed energy gradient from proximal to distal in Rampur shale onwards.

carbonate sediments on the hanging wall were reworked and transported to a mud-depositing environment by high-energy flows such as storms (Fig. 10a). Coarse arenaceous intervals with grain size ranging from boulder and/or pebbly to medium sand alternate with other shale units. As well as demonstrating a wide variation in grain size, these units also vary in their depositional character and environmental settings. The conglomeratic and granule-bearing feldspathic sandstone wedge at the lower part of the Koldaha shale shows a clear imprint for the base-of-slope delta formed at the margin of a fault scarp due to the activation of the basin margin fault following the deposition of porcellanite. This is evident from the presence of angular boulders and pebbles of underlying lithology, namely porcellanite, shale and sandstones of Deoland within conglomerate. The faulted margin possibly acted as the footwall for the Koldaha half-graben basin, which triggered the supply of coarse detritus in the form of a fan and also caused large-scale subsidence in the basin near the footwall (Fig. 10b). The occurrence of disparately thick distal shelf shale (dark-grey to greenish shale) immediately above the fan deposit corroborates this idea. However, the other two inferred fluvial arenaceous units with W-wards palaeocurrent and wedge-out direction suggest the operation of fluvial systems from the eastern side, that is, the hanging wall of the Koldaha rift basin, and thus support the half-graben model for Koldaha shale deposition. (Fig. 10b; cf. Leeder & Gawthorpe, 1987; Lambiase, 1990). The emplacement of fluvial systems on the Koldaha shelf at two stratigraphic levels indicates a relative fall in sea level and its emergence and subsequent development of intraformational unconformity (Bose *et al.* 1997; Samanta *et al.* 2016). Unlike Koldaha shale, Rampur shale shows a uniform fining- and thinning-upwards character, indicating an overall transgressive depositional motif, as it was deposited on a quiet shelf ranging in bathymetry from inner to outer shelf. The quiet shelf setting was achieved with attenuation of rift tectonics in the basin following the deposition of the Koldaha shale (Bose *et al.* 1997; Fig. 10c). However, as with shelves in other time domains, the Rampur shelf was also infested by storm currents (Sarkar *et al.* 2002*a*; AK Singh, unpub. PhD thesis, University of Delhi, 2015).

Unlike the lower Vindhyan shales that were mostly deposited under the influence of rift tectonics, the Bijaygarh shale of the upper Vindhyan was deposited in a stable shelf with a coarsening- and thickening-upwards progradational depositional motif. Commencing its sedimentation as pyritiferous black shale in an anoxic distal shelf setting, the Bijaygarh shelf prograded to a sandstone–shale package of inner shelf – distal shoreface setting (Fig. 10d). A mutual relation between gutters and wave ripples within the storm-originated beds of the Bijaygarh shale allowed the documentation of a geostrophic current on the Bijaygarh shelf. The multi-storied, fining-upwards poorly sorted arenaceous packages that intercept the Rewa shale succession at multiple stratigraphic levels, with (1) distinctive lenticular bed geometry and (2) conglomeratic lag enriched in pebbly oxidized rip-up mud clasts, bear a clear indication for the incursion of fluvial systems onto the shelf, at least up to the inner shelf at different time intervals in the course of sedimentation of the Rewa shale (Figs 7a, 10e). Unlike all shale units, sedimentation in the Sirbu shale initiated in a peritidal setting as evident from the occurrence of carbonate lithounits, which later transformed into a shelf-like setting where depositional settings ranged from storm-influenced inner to outer

https://doi.org/10.1017/S0016756820001168 Published online by Cambridge University Press

shelf (Fig. 10f). The properties of the singular arenaceous bed (*c.* 35 cm thick) present within the Sirbu shale succession – sharp upper and lower boundaries, normal grading, rip-up mud-pebble conglomerate at the base and Bouma T_{abc} cycles – indicate its event-based origin by the operation of an erosive and waning turbiditic flow onto the Sirbu shelf, in which deposition occurred in essentially starved shelf conditions as evident from the prolific growth of bacterial mat. A possible climatic and/or tectonic pulse led to mass failure in the proximal part, and may have triggered a turbiditic flow and deposited the sandstone bed in a distal starved shelf. From the above discussion, the coarse arenaceous beds (sandstone and/or conglomerate) within the Vindhyan shale successions are products of different processes that operated on an event- to basin-scale. However, their occurrence is not unequivocal evidence of a fall in relative sea level, and they do not display the same depositional mechanism as such a process.

4.b. Clues about basin tectonics

In the absence of high-resolution geophysical data, workers have relied heavily on process-based physical sedimentology (Bose *et al.* 1997, 2001; Sarkar *et al.* 2002*a*; *b*; Chakraborty, 2006; Chakraborty *et al.* 2012) and sediment geochemistry (Chakrabarti *et al.* 2007; Paikaray *et al.* 2008; Shukla *et al.* 2019) for the extrapolation of tectonic controls on the evolution of the Vindhyan Basin. The decades of study, although under debate and inconclusive, have projected widely varying tectonic models extending from an intracratonic setting (Chanda & Bhattacharyya, 1982; Soni *et al.* 1987), to a foreland setting (Chakraborty & Bhattacharyya, 1996; Chakrabarti *et al.* 2007; Shukla *et al.* 2019) to a temporarily evolved rift-sag setting (Sarkar *et al.* 1995; Bose *et al.* 1997, 2001; Sarkar *et al.* 2002*b*). In particular, trace-element data, Nd isotope-based studies and seismic reflection studies (Chakrabarti *et al.* 2007; Mandal *et al.* 2018; Shukla *et al.* 2019) speculate on the initiation of the Vindhyan basin as a foreland basin with the existence of a subduction-related arc system. Interestingly, proponents of a foreland setting differ in their subduction model. Chakrabarti *et al.* (2007) and Shukla *et al.* (2019) conceived subduction of the Bundelkhand craton under the Bastar and Aravalli cratons; however, from consideration of seismic reflection stack imaging, Mandal *et al.* (2018) suggested the opening of the Vindhyan Basin in an extensional strike-slip mode that followed subduction and collision between the Bundelkhand craton and the Mewar craton. However, none of these studies supported their claims with field-based documentation such as the basin-scale variation in stratigraphic thickness of different formations and the pervasive northwesterly palaeocurrent from different stratigraphic levels of the Vindhyan succession present in the Son valley.

Our field-based sedimentology from argillaceous intervals suggests rift-guided sedimentation in the Vindhyan Basin up to the time of deposition of the Koldaha shale, which later transformed into sag tectonics during the deposition of the upper Vindhyans and thereby supports the tectonic model proposed by Bose *et al.* (2001) (Figs 2–4,10a, b). The occurrence of basin instability structures such as slumps, small-scale listric faults, conjugate faults, contorted beds and joints within the Koldaha shale are indicative of horizontal-extension-related regional tectonics (Sarkar *et al.* 1995; Bose *et al.* 1997; AK Singh, unpub. PhD thesis, University of Delhi, 2015; Samanta *et al.* 2016). The small-scale deformation structures observed at various stratigraphic levels of the Kajrahat Formation and Koldaha shale bear indication of a SW-wards regional slope, whereas large-scale normal faults with conglomeratic fan delta sediments at their toes point to a persistent NE-wards dipping slope. An almost E–W-elongated basin, flanked by two converging slopes dipping towards each other, is inferred (Bose *et al.* 1997). The very-coarse-grained conglomeratic sediments within the Koldaha shale containing angular clasts of underlying rock deposited on the western flank suggest the existence of a very steeply sloped gradient, whereas comparatively finer-grained fluvial sediments on the eastern flank indicate the presence of a much gentler slope. The existence of a steep western flank along with a gentle eastern slope is evidence of a half-graben-like tectonic setting for the deposition of the Lower Vindhyans up to the Koldaha shale (Fig. 10b).

Our idea is supported by a seismic sounding study (Kaila *et al.* 1989) that identified block tectonics as an active mechanism throughout the geological history of the basin. The continuation of such an extensional regime can also be corroborated by the depositional cycles recorded within Arangi and Koldaha shales (Figs 2a, b, 3a–c, 4a, b; Bose *et al.* 2001; AK Singh, unpub. PhD thesis, University of Delhi, 2015). The fact that the transition from rift to sag stage occurred immediately after the deposition of the Koldaha shale is evident from significant lateral facies continuity from the Rampur shale onwards, and can also be observed in the argillaceous intervals of the Upper Vindhyan (Fig. 10c–f). The progradational cycles within the Sirbu shale, punctuated by soft sediment deformation structures (slump fold, slump scar, slide plane, etc.) in the topmost sand bed of these cycles indicate episodic subsidence of the basin floor and the creation of basin accommodation. The decades of study have therefore refined our outlook on tectonic evolution of the Vindhyan Basin, although further authentication and augmentation seems warranted on the basis of high-resolution basin-scale subsurface geophysics.

5. Conclusion

In combining data from the existing literature with the addition of new process-based sedimentary data, this paper critically examines six different shale members (Arangi, Koldaha, Rampur, Bijaygarh, Rewa and Sirbu) of the Vindhyan Supergroup exposed in the Son Valley, central India and attempts to understand the depositional dynamics operative on the Vindhyan shelf. It is inferred that Vindhyan shales were deposited largely in a marine-shelf environment with relative bathymetry ranging from inner (near to fair-weather wave base) to distal (below storm wave base) shelf conditions. The depositional history of Koldaha, Rewa and Sirbu shales was punctuated by thick arenaceous intervals interpreted as fan delta and braided fluvial deposition during the intermittent sea-level lowstand, or as event deposition during sea-level highstand. It is also evident that the Vindhyan shelf was storm-infested throughout its sedimentation history, as each shale unit exhibits the profuse presence of gutters, prod marks, skip marks, hummocks and wave ripples (except for the Arangi shale, which records deposition below storm wave base). The mutual orientation of flow vectors (gutters, prods and wave ripples) also provided clues regarding the operations of both storm return flow and geostrophic current on the Vindhyan shelf. The sediment stacking pattern and depositional cycles record fining-upwards transgressive depositional systems for Arangi and Rampur shale, whereas the thinning- and fining-upwards (retrogradational) as well as thickening- and coarsening-upwards (progradational) stacking patterns are indicative of the transgressive and highstand regressive depositional history described by the Koldaha, Bijaygarh, Rewa and Sirbu shales.

https://doi.org/10.1017/S0016756820001168 Published online by Cambridge University Press

Acknowledgements. AKS is grateful to the director, Birbal Sahni Institute of Palaeosciences, Lucknow for providing necessary facilities and permission (BSIP/RDCC/Publication no. 14/2020-21) to publish this manuscript. PPC acknowledges funding from the Department of Science and Technology (DST), New Delhi and infrastructural facility from the Department of Geology, University of Delhi. Research funding from the Council of Scientific and Industrial Research (CSIR) and the University of Delhi is also gratefully acknowledged. Professor Patrick Eriksson and an anonymous reviewer are also thanked for their constructive reviews.

Conflict of interest. None.

References

Arnott RWC (1993) Quasi-planar laminated sandstone beds of the lower Cretaceous Bootlegger member, north-central Montana: evidence of combined flow sedimentation. *Journal of Sedimentary Petrology* **63**, 488–94.

Auden JB (1933) *Vindhyan Sedimentation in the Son Valley, Mirzapur District*. pp. 141–250. Geological Survey of India, Calcutta, Memoir no. 62, part 2.

Banerjee I (1996) Populations, trends and cycles in combined flow bedforms. *Journal of Sedimentary Research* **66**, 868–74.

Banerjee S (2000) Climatic versus tectonic control on storm cyclicity in Mesoproterozoic Koldaha Shale, central India. *Gondwana Research* **3**, 521–28.

Banerjee S and Jeevankumar S (2003) Facies motif and paleogeography of Kheinjua Formation, Vindhyan Supergroup, eastern Son valley. *Gondwana Geological Magazine* Special Volume **7**, 363–70.

Banerjee S and Jeevankumar S (2005) Microbially originated wrinkle structures on sandstones and their stratigraphic context: Paleoproterozoic Koldaha Shale, central India. *Sedimentary Geology* **176**, 211–24.

Bera MK, Sarkar A, Chakraborty PP, Loyal RS and Sanyal P (2008) Marine to continental transition in Himalayan foreland. *Geological Society of America Bulletin* **120**, 1214–32.

Boggs S Jr (2006) *Principles of Sedimentology and Stratigraphy* (4th ed.). New Jersey: Pearson Prentice Hall, 662 p.

Bose PK, Banerjee S and Sarkar S (1997) Slope-controlled seismic deformation and tectonic framework of deposition: Koldaha Shale, India. *Tectonophysics* **269**, 151–69.

Bose PK, Chakraborty S and Sarkar S (1999) Recognition of ancient eolian longitudinal dunes: a case study in Upper Bhander Sandstone, Son valley, India. *Journal of Sedimentary Research* **69**, 86–95.

Bose PK and Chanda SK (1986) Storm deposits and hummocky cross-stratification: a geological viewpoint. *Quarterly Journal of Geological Mining and Metallurgical Society of India* **58**, 53–68.

Bose PK and Chaudhuri A (1990) Tide versus storm in epeiric coastal deposition: two Proterozoic sequences, India. *Geological Journal* **25**, 81–101.

Bose PK, Chaudhuri AK and Seth A (1988) Facies, flow and bedform pattern across a storm-dominated inner continental shelf: Proterozoic Kaimur Formation, Rajasthan, India. *Sedimentary Geology* **59**, 275–93.

Bose PK, Sarkar S, Chakraborty S and Banerjee S (2001) Overview of the Meso- to Neoproterozoic evolution of the Vindhyan basin, central India. *Sedimentary Geology* **141**, 395–419.

Bose PK, Sarkar S, Das NG, Banarjee S, Mandal A and Chakraborty N (2015) Proterozoic Vindhyan Basin: configuration and evolution. In *Precambrian Basins of India: Stratigraphic and Tectonic Context* (eds R Mazumdar and PG Eriksson), pp. 85–102. Geological Society of London, Memoir no. 43.

Bouma AH (1962) *Sedimentology of Some Flysch Deposits*. Amsterdam: Elsevier Publishing Company, 168 p.

Bourgeois J (1980) A transgressive shelf sequence exhibiting hummocky cross-stratification: the Cape Sebastian Sandstone (Upper Cretaceous), Southwestern Oregon. *Journal of Sedimentary Petrology* **50**, 681–702.

Brenchley PJ and Newall G (1982) Storm-influenced innershelf sand lobes in the Caradoc (Ordovician) of Shropshire, England. *Journal of Sedimentary Petrology* **52**, 1257–69.

Carvajal CR and Steel RJ (2006) Thick turbidite successions from supply dominated shelves during sea level highstand. *Geology* **34**, 665–68.

Catuneanu O (2017) Sequence stratigraphy: guidelines for a standard methodology. *Stratigraphy & Timescales* **2**, 1–57.

Catuneanu O, Bhattacharya JP, Blum MD, Dalrymple RW, Eriksson PG, Fielding CR, Fisher WL, Galloway WE, Gianolla P, Gibling MR, Giles KA, Holbrook JM, Jordan MR, Kendall CGStC, Macurda B, Martinsen OJ, Miall AD, Nummedal D, Posamentier HW, Pratt BR, Shanley KW, Steel RJ, Strasser A and Tucker ME (2010) Sequence stratigraphy: common ground after three decades of development. *First Break* **28**, 21–34.

Chakrabarti R, Basu AR and Chakrabarti A (2007) Trace element and Nd-isotopic evidence for sediment sources in the mid-Proterozoic Vindhyan Basin, central India. *Precambrian Research* **159**, 260–74.

Chakraborty C (1995) Gutter casts from the Proterozoic Bijaygarh Shale Formation, India: their implication for storm-induced circulation in shelf settings. *Geological Journal* **30**, 69–78.

Chakraborty C (2006) Proterozoic intracontinental basin: the Vindhyan example. *Journal of Earth System Science* **115**, 3–22.

Chakraborty C and Bhattacharyya A (1996) Fan-delta sedimentation in a foreland moat: Deoland Formation, Vindhyan Supergroup, Son valley. In *Recent Advances in Vindhyan Geology* (ed. A Bhattacharya), pp. 27–48. Geological Society of India, Bangalore, Memoir no. 36.

Chakraborty C and Bose PK (1992) Rhythmic shelf storm beds: Proterozoic Kaimur Formation, India. *Sedimentary Geology* **77**, 259–68.

Chakraborty PP (2004) Facies architecture and sequence development in a Neoproterozoic carbonate ramp: Lakheri Limestone Member, Vindhyan Supergroup, central India. *Precambrian Research* **132**, 29–53.

Chakraborty PP (2006) Outcrop signatures of relative sea level fall on a siliciclastic shelf: examples from the Rewa Group of Proterozoic Vindhyan basin. *Journal of Earth System Science* **115**, 23–36.

Chakraborty PP, Banerjee S, Das NG, Sarkar S and Bose PK (1996) Volcaniclastics and their sedimentological bearing in Proterozoic Kaimur and Rewa Groups in central India. In *Recent Advances in Vindhyan Geology* (ed. A Bhattacharya), pp. 59–76. Geological Society of India, Bangalore, Memoir no. 36.

Chakraborty PP, Das P, Das K, Saha S and Balakrishnan S (2012) Regressive depositional architecture on a Mesoproterozoic siliciclastic ramp: sequence stratigraphic and Nd isotopic evidences from Bhalukona Formation, Singhora Group, Chhattisgarh Supergroup, central India. *Precambrian Research* **200**, 129–48.

Chakraborty PP, Pant NC and Paul P (2015) Controls on sedimentation in Indian Palaeoproterozoic basins: clues from the Gwalior and Bijawar basins, central India. In *Precambrian Basins of India: Stratigraphic and Tectonic Context* (eds R Mazumdar and PG Eriksson), pp. 67–83. Geological Society of London, Memoir no. 43.

Chakraborty PP and Paul S (2008) Forced regressive wedges on a Neoproterozoic siliciclastic shelf: Chandarpur Group, central India. *Precambrian Research* **162**, 227–47.

Chakraborty PP, Sarkar A, Das K and Das P (2009) Alluvial fan to storm-dominated shelf transition in the Mesoproterozoic Singhora Group, Chhattisgarh Supergroup, Central India. *Precambrian Research* **170**, 88–106.

Chakraborty PP and Sarkar S (2005) Episodic emergence of offshore shale and its implication: late Proterozoic Rewa Shale, Son Valley, central India. *Journal of Geological Society of India* **66**, 699–712.

Chakraborty PP, Sarkar S and Bose PK (1998) A viewpoint on intracratonic chenier evolution: clue from a reappraisal of the Proterozoic Ganurgarh Shale, Central India. In *The Indian Precambrian* (ed. BS Paliwal), pp. 61–72. Jodhpur: Scientific Publishers India.

Chakraborty T and Chaudhuri AK (1990) Stratigraphy of the late Proterozoic Rewa Group and paleogeography of the Vindhyan basin in central India during Rewa sedimentation. *Journal of Geological Society of India* **36**, 383–402.

Chanda SK and Bhattacharyya A (1982) Vindhyan sedimentation and paleogeography: post-Auden developments. In *Geology of Vindhyanchal* (eds KS Valdiya, SB Bhatia and VK Gaur), pp. 88–101. New Delhi: Hindusthan Publishing Corporation.

Chandler FW (1984) Sedimentary setting of an early Proterozoic copper occurrence in the Cobalt Group, Ontario: a preliminary assessment in current research. *Geological Survey of Canada* **84**, 185–92.

Cloeting S (1988) Intraplate stresses: a new element in basin analysis. In *New Perspectives in Basin Analysis* (eds KL Kleinspehn and C Paola), pp. 205–30. New York: Springer-Verlag.

Crawford AR and Compston W (1969) The age of the Vindhyan system of Peninsular India. *Quarterly Journal of the Geological Society* **125**, 351–71.

De C (2003) Possible organisms similar to Ediacaran forms from the Bhander Group, Vindhyan Supergroup, late Neoproterozoic of India. *Journal of Asian Earth Sciences* **21**, 387–95.

De C (2006) Ediacara fossil assemblage in the upper Vindhyans of Central India and its significance. *Journal of Asian Earth Sciences* **27**, 660–83.

Dott RH (1996) Episodic event deposits versus stratigraphic sequences- shall the twain never meet? *Sedimentary Geology* **104**, 243–47.

Dott RH and Bourgeois J (1982) Hummocky stratification: significance of its variable bedding sequences. *Geological Society of American Bulletin* **93**, 663–80.

Duke WL (1985) Hummocky cross-stratification, tropical hurricanes, and intense winter storms. *Sedimentology* **32**, 167–94.

Duke WL, Arnott RW and Cheel RJ (1991) Shelf sandstones and hummocky cross-stratification: new insights on a stormy debate. *Geology* **9**, 625–28.

Eriksson PG, Condie KC, Tirsgaard H, Mueller WU, Altermann W, Miall AD, Aspler LB, Catuneanu O and Chiarenzelli JR (1998) Precambrian clastic sedimentation systems. *Sedimentary Geology* **120**, 5–53.

Eriksson PG, Mazimdar R, Sarkar S, Bose PK, Altermann W and Van der Marwe R (1999) The 2.7–2.0 Ga volcano-sedimentary record of Africa, India and Australia: evidence for global and local changes in sea level and continental freeboard, *Precambrian Research* **97**, 269–302.

Gopalan K, Kumar A, Kumar S and Vijayagopal B (2013) Depositional history of the Upper Vindhyan succession, central India: time constraints from Pb–Pb isochron ages of its carbonate components. *Precambrian Research* **233**, 108–17.

Gregory LC, Meert JG, Pradhan V, Pandit MK, Tamrat E and Malone SJ (2006) A paleomagnetic and geochronologic study of the Majhgawan Kimberlite, India: implications for the age of the Vindhyan Supergroup. *Precambrian Research* **149**, 65–75.

Grotzinger JP (1986) Cyclicity and paleoenvironmental dynamics: Rocknest platform, northwest Canada. *Geological Society of America Bulletin* **97**, 1208–31.

Grotzinger JP (1989) Construction of early Proterozoic (1.9 Ga) barrier reef complex, Rocknest platform, Northwest Territories. In *Reef: Canada and Adjacent Areas* (eds HHJ Geldsetzer, NP James and GE Tebbutt), pp. 30–37. Canadian Society of Petroleum Geologists, Calgary, Memoir no. 13.

Gupta S, Jain KC, Srivastava VC and Mehrotra RD (2003) Depositional environment and tectonism during the sedimentation of the Semri and Kaimur Groups of rocks, Vindhyan Basin. *Journal of Palaeontological Society of India* **48**, 181–90.

Hamblin AP and Walker RG (1979) Storm dominated shallow marine deposits: the Fernie-Kootenay (Jurassic) transition, Southern Rocky Mountains. *Canadian Journal of Earth Science* **16**, 1673–90.

Hamon Y and Merzeraud G (2008) Facies architecture and cyclicity in a mosaic carbonate platform: effects of fault-block tectonics (Lower Lias, Causses platform, south-east France). *Sedimentology* **55**, 155–78.

Harms JC, Southard JB, Spearing DR and Walker RG (1975) *Depositional Environments as Interpreted from Primary Sedimentary Structures and Stratification Sequences*. Tulsa: Society for Sedimentary Geology, Short Course 2, 166 p.

Harms JC, Southard JB and Walker RG (1982) Structures and Sequences in Clastic Rocks. Tulsa: Society for Sedimentary Geology, Short Course 9.

Hunter RE and Clifton HE (1982) Cyclic deposits and hummocky cross-stratification of probable storm origin in Upper Cretaceous rocks of Cape Sebastian area, southwest Oregon. *Journal of Sedimentary Petrology* **52**, 127–43.

Jackson MJ, Simpson EL and Eriksson KA (1990) Facies and sequence stratigraphic analysis in an intracratonic, thermal-relaxation basin: the Early Proterozoic, Lower Quilalar Formation and Ballara Quartzite, Mount Isa Inlier, Australia. *Sedimentology* **37**, 1053–78.

Jones AT, Frank TD and Fielding CR (2006) Cold climate in the eastern Australian mid to late Permian may reflect cold upwelling waters. *Palaeogeography, Palaeoclimatology, Palaeoecology* **237**, 370–77.

Kaila KL, Murty PR and Mall DM (1989) The evolution of the Vindhyan basin vis-a-vis the Narmada-Son lineament, central India, from deep seismic soundings. *Tectonophysics* **162**, 277–89.

Kale VS and Phansalkar VG (1991) Purana basins of Peninsular India: a review. *Basin Research* **3**, 1–36.

Kasanzu C, Maboko MAH and Manya S (2008) Geochemistry of fine-grained clastic sedimentary rocks of the Neoproterozoic Ikorongo Group, NE Tanzania: implications for provenance and source rock weathering. *Precambrian Research* **164**, 201–13.

Kidwell SM (1991) Condensed deposits in siliciclastic sequences: expected and observed features. In *Cycles and Events in Stratigraphy* (eds G Einseile, W Ricken and A Seilacher), pp. 682–95. Berlin: Springer-Verlag.

Krishnan MS (1968) *Geology of India and Burma*. New Delhi: Tata McGraw Hill Publication. 536 p.

Krishnan MS and Swaminath J (1959) The Great Vindhyan Basin of northern India. *Journal of Geological Society of India* **1**, 10–36.

Kuehl SA, Hariu TM and Moore WS (1989) Shelf sedimentation off the Ganges–Brahmaputra river system: evidence for sediment bypassing to the Bengal fan. *Geology* **17**, 1132–35.

Kumar A, Kumari VP, Dayal AM, Murthy DS and Gopalan K (1993) Rb-Sr ages of Proterozoic kimberlites of India: evidence for contemporaneous emplacement. *Precambrian Research* **62**, 227–37.

Kumar S and Srivastava P (1997) A note on the carbonaceous megafossils from the Neoproterozoic Bhander Group, Maihar area, Madhya Pradesh. *Journal of the Palaeontological Society of India* **42**, 1–46.

Kumar S and Srivastava P (2003) Carbonaceous megafossils from the Neoproterozoic Bhander Group, Central India. *Journal of the Palaeontological Society of India* **48**, 139–54.

Lambiase JJ (1990) A model for tectonic control of lacustrine stratigraphic sequences in continental rift basins. In *Lacustrine Exploration: Case Studies and Modern Analogs* (ed. B Katz), pp. 265–76. American Association of Petroleum Geologists, Tulsa, Memoir no. 50.

Leeder MR and Gawthorpe RL (1987) Sedimentary models for extensional tilt block/half graben basins. In *Continental Extensional Tectonics* (eds MP Coward, JF Dewey and PL Hancock), pp. 139–52. Geological Society of London, Special Publication no. 28.

Lindsey KA and Gaylord DR (1992) Fluvial, coastal, nearshore, and shelf deposition in the Upper Proterozoic (?) to Lower Cambrian Addy Quartzite, northeastern Washington. *Sedimentary Geology* **77**, 15–35.

Long DGF (2011) Katherine Group. Section 3.1.3. In *Geology of the Central Makenzie Mountains of the Northern Canadian Cordillera* (eds E Martel, EC Turner and B Fisher), pp. 39–56. Northwest Territories Geological Survey, Yellowhammer, Special Volume **1**.

Lowe DR (1982) Sediment gravity flows: II. Depositional models with special reference to the deposits of high density turbidity currents. *Journal of Sedimentary Petrology* **52**, 279–97.

Malone SJ, Meert JG, Banerjee DM, Pandit MK, Tamrat E, Kamenov GD, Pradhan VR and Sohl LE (2008) Paleomagnetism and detrital zircon geochronology of the upper Vindhyan sequence, Son Valley and Rajasthan, India: a ca. 1000 Ma closure age for the Purana basins? *Precambrian Research* **164**, 137–59.

Mandal B, Vaidya VR, Sen MK, Periyasamy K and Sarkar D (2018) Common reflection surface stack imaging of the Proterozoic Chambal valley Vindhyan basin and its boundary fault in the northwestern India: constraints on crustal evolution and basin formation. *Tectonics* **37**, 1393–410.

Mandal S, Choudhuri A, Mondal I, Sarkar S, Chakraborty PP and Banerjee S (2019) Revisiting the boundary between the Lower and Upper Vindhyan, Son valley, India. *Journal of Earth System Science* **128**, 222.

Mazumder R, Bose PK and Sarkar S (2000) A commentary on the tectono sedimentary record of the pre-2.0 Ga continental growth of India vis-a-vis a possible pre-Gondwana Afro-Indian subcontinent. *Journal of African Earth Science* **30**, 201–17.

Miall AD (2000) *Principles of Sedimentary Basin Analysis*. New York: Springer-Verlag. 616 p.

Mondal MEA, Goswami JN, Deomurari MP and Sharma KK (2002) Ion microprobe 207Pb/206Pb ages of zircons from the Bundelkhand Massif, northern India: implications for crustal evolution of the Bundelkhand–Aravalli supercontinent. *Precambrian Research* **117**, 85–100.

Mulder T and Alexander J (2001) The physical character of subaqueous sedimentary density flows and their deposits. *Sedimentology* **48**, 269–99.

https://doi.org/10.1017/S0016756820001168 Published online by Cambridge University Press

Myrow PM (1992) Pot and gutter casts from the Chapel Island Formation, southeast Newfoundland. *Journal of Sedimentary Petrology* **63**, 992–1007.

Myrow PM and Southard JB (1996) Tempestite deposition. *Journal of Sedimentary Research* **66**, 875–87.

Nelson CH (1982) Modern shallow-water graded sand layers from storm surges, Bering Shelf: a mimic of Bouma sequences and turbidite systems. *Journal of Sedimentary Petrology* **52**, 537–45.

Nemec W and Steel RJ (1984) Alluvial and coastal conglomerates: their significant features and some comments on gravelly mass-flow deposits. In *Sedimentology of Gravels and Conglomerates* (eds EH Koster and RJ Steel), pp. 1–31. Canadian Society of Petroleum Geologists, Calgary, Memoir no. 10.

Okada H and Ohta S (1993) Photographic evidence for bottom current activity in the Suruga and Sagami Bays, central Japan. *Sedimentary Geology* **82**, 103–32.

Paikaray S, Banerjee S and Mukherji S (2008) Geochemistry of shales from the Paleoproterozoic to Neoproterozoic Vindhyan Supergroup: implications on provenance, tectonics and paleoweathering. *Journal of Asian Earth Sciences* **32**, 34–48.

Patranabis-Deb S (2004) Lithostratigraphy of the Neoproterozoic Chhattisgarh sequence: it's bearing on the tectonics and paleogeography. *Gondwana Research* **7**, 323–37.

Pivnik DA (1990) Thrust-generated fan-delta deposition: Little Muddy Creek Conglomerate, SW Wyoming. *Journal of Sedimentary Petrology* **60**, 489–503.

Posamentier HW and Vail PR (1988) Eustatic controls on clastic deposition II - Sequence and system tract models. In *Sea Level Changes: An Integrated Approach* (eds CK Wilgus, BS Hastings, CGSC Kendall, HW Posamentier, CA Ross and JC Van Wagoner), pp. 125–54. SEPM (Society for Sedimentary Geology), Tulsa, Special Publication no. 42.

Postma G (1984) Mass-flow conglomerates in a submarine canyon: Abrioja fandelta, Pliocene, southeast Spain. In *Sedimentology of Gravels and Conglomerates* (eds EH Koster and RJ Steel), pp. 237–58. Canadian Society of Petroleum Geologists, Calgary, Memoir no. 10.

Postma G and Drinia G (1993) Architecture and sedimentary facies evolution of a marine, expanding outer-arc half-graben (Crete, late Miocene). *Basin Research* **5**, 103–24.

Potter PE, Mynard JB and Depetris PJ (2005) *Mud and Mudstone*. New York: Springer Verlag, 297 p.

Prasad B (2007) *Obruchevella* and other terminal Proterozoic (Vendia) organic-walled microfossils from the Bhander Group (Vindhyan Supergroup), Madhya Pradesh. *Journal of Geological Society of India* **69**, 295–310.

Pratt BR, James NP and Cowan CA (1992) Peritidal carbonates. In *Facies Models: Response to Sea Level Change*, 3rd ed. (eds RG Walker and NP James), pp. 303–22. St John's: Geological Association of Canada.

Preiss WV and Forbes BG (1981) Stratigraphy, correlation and sedimentary history of Adelandean (Late Proterozoic) basins of Australia. *Precambrian Research* **15**, 255–304.

Rai V, Shukla M and Gautam R (1997) Discovery of carbonaceous megafossils (Chuaria-Tawuia assemblage) from the NeoproterozoicVindhyan succession (Rewa Group), Allahabad–Rewa area, India. *Current Science* **73**, 783–88.

Ramakrishnan M and Vaidyanadhan R (2010) *Geology of India* (Vol. **1**). Bangalore: Geological Society of India Publications, 556 p.

Rasmussen B, Bose PK, Sarkar S, Banerjee S, Fletcher IR and McNaughton NJ (2002) 1.6Ga U–Pb zircon age for the Chorhat Sandstone, Lower Vindhyan, India: possible implications for the early evolution of animals. *Geology* **20**, 103–106.

Ray JS, Martin MW, Veizer J and Bowring SA (2002) U–Pb zircon dating and Sr isotope systematics of the Vindhyan Supergroup, India. *Geology* **30**, 131–34.

Ray JS, Veizer J and Davis WJ (2003) C, O, Sr and Pb isotope systematics of carbonate sequences of the Vindhyan Supergroup, India: age, diagenesis, correlations and implications for global events. *Precambrian Research* **121**, 103–40.

Roger S, Feraud G, de Beaulieu JL, Thouveny N, Coulon C, Cocheme JJ, Andrieu V and Williams T (1999) $^{40}Ar/^{39}Ar$ dating on tephra of the Velay maars (France); implications for the late Pleistocene proxy-climatic record. *Earth Planetary Science Letters* **170**, 287–99.

Roy AB (1988) Stratigraphic and tectonic framework of the Aravalli Mountain range. In *Precambrian of the Aravalli Mountain, Rajasthan, India* (ed. AB Roy), pp. 3–32. Geological Society of India, Bangalore, Memoir no. 7.

Samanta P, Mukhopadhyay S and Eriksson PG (2016) Forced regressive wedge in the Mesoproterozoic Koldaha shale, Vindhyan basin, Son valley, central India. *Marine and Petroleum Geology* **71**, 329–43.

Samanta P, Mukhopadhyay S, Mondal A and Sarkar S (2011) Microbial mat structures in profile: the Neoproterozoic Sonia Sandstone. *Journal of Asian Earth Science* **40**, 542–49.

Sarangi S, Gopalan K and Kumar S (2004) Pb–Pb age of earliest megascopic eukaryotic alga bearing Rohtas Formation, Vindhyan Supergroup, India: implications for Precambrian atmospheric oxygen evolution; *Precambrian Research* **132**, 107–21.

Sarkar A, Chakraborty PP, Mishra B, Bera MK, Sanyal P and Paul S (2010) Mesoproterozoic sulphidic ocean, delayed oxygenation and evolution of early life: sulphur isotope clues from Indian Proterozoic basins. *Geological Magazine* **147**, 206–18.

Sarkar A, Sengupta SM, McArthur JM, Ravenscroft P, Bera MK, Bhushan R, Samanta A and Agrawal S (2009) Evolution of Ganges–Brahmaputra western delta plain: clues from sedimentology and carbon isotopes. *Quaternary Science Reviews* **28**, 2564–81.

Sarkar S, Banerjee S and Chakraborty S (1995) Synsedimentary seismic signature in Mesoproterozoic Koldaha Shale, Kheinjua Formation, central India. *Indian Journal of Earth Science* **22**, 158–64.

Sarkar S, Banerjee S, Chakraborty S and Bose PK (2002a) Shelf storm flow dynamics: insight from the Mesoproterozoic Rampur Shale, central India. *Sedimentary Geology* **147**, 89–104.

Sarkar S, Banerjee S, Eriksson PG and Catuneanu O (2005) Microbial mat control on siliciclastic Precambrian sequence stratigraphic architecture: examples from India. *Sedimentary Geology* **176**, 195–209.

Sarkar S, Banerjee S, Samanta P, Chakraborty N, Chakraborty PP, Mukhopadhyay S and Singh AK (2014) Microbial mat records in siliciclastic rocks: examples from four Indian Proterozoic basins and their modern equivalents in Gulf of Cambay. *Journal of Asian Earth Sciences* **91**, 362–77.

Sarkar S and Bose PK (1992) Variations in Proterozoic stromatolites over a transition from basin plain to near shore subtidal zone. *Precambrian Research* **56**, 139–57.

Sarkar S, Chakraborty PP and Bose PK (1996) Proterozoic Lakheri Limestone, Central India: facies, paleogeography and physiography. In *Vindhyans: Recent Advances in Vindhyan Geology* (ed. A Bhattacharyya), pp. 5–25. Geological Society of India, Bangalore, Memoir no. 36.

Sarkar S, Chakraborty S, Banerjee S and Bose PK (2002b) Facies sequence and cryptic imprint of sag tectonics in late Proterozoic Sirbu Shale, central India. In *Precambrian Sedimentary Environments: A Modern Approach to Ancient Depositional Systems* (eds W Altermann and P Corcoran), pp. 369–82. International Association of Sedimentologists, Special Publication no. 33.

Schieber J (1986) The possible role of benthic microbial mats during the formation of carbonaceous shales in shallow Mid-Proterozoic basins. *Sedimentology* **33**, 521–36.

Schieber J (1989) Facies and origin of shales from the Mid- Proterozoic Newland Formation, Belt Basin, Montana, USA. *Sedimentology* **36**, 203–19.

Schieber J (1990) Significance of styles of epicontinental shales sedimentation in the Belt, Mid-Proterozoic of Montana, USA. *Sedimentary Geology* **69**, 297–312.

Schieber J (1991) Sedimentary structures: Textures and depositional settings of shales from the lower Belt Supergroup, mid–Proterozoic Montana, USA. In *Microstructure of Fine-Grained Sediments* (eds RH Bennett, WR Bryant and MH Hulbert), pp. 101–108. New York: Springer-Verlag.

Schieber J (1998) Possible indicators of microbial mat deposits in shales and sandstones: examples from the Mid-Proterozoic Belt Supergroup, Montana, USA. *Sedimentary Geology* **24**, 105–124.

Schieber J (1999) Microbial mats in terrigenous clastics; the challenge of identification in the rock record. *Palaios* **14**, 3–12.

https://doi.org/10.1017/S0016756820001168 Published online by Cambridge University Press

Schieber J (2016) Mud re-distribution in epicontinental basins – exploring likely processes. *Marine and Petroleum Geology* **71**, 119–33.

Shanmugam G (2006) The tsunamite problem. *Journal of Sedimentary Research* **76**, 718–30.

Shanmugam G, Poffenberger M and Toro Alava J (2000) Tide-dominated estuarine facies in the Hollin and Napo ("T" and "U") formations (Cretaceous) Sacha Field, Oriente Basin, Ecuador. *American Association of Petroleum Geologists Bulletin* **84**, 652–82.

Shukla AD, George BG and Ray JS (2019) Evolution of the Proterozoic Vindhyan Basin, Rajasthan, India: insights from geochemical provenance of siliciclastic sediments. *International Geology Review* **62**, 153–67.

Singh A, Anand V, Pandey P and Chakraborty PP (2013) Nodular features from Proterozoic Sonia Sandstone, Jodhpur Group, Rajasthan: a litho-biotectonic perspective. *Journal of Earth System Science* **122**, 309–20.

Singh AK, Chakraborty PP and Sarkar S (2018) Redox structure of Vindhyan hydrosphere: clues from total organic carbon, transition metal (Mo, Cr) concentrations and stable isotope (delta C-13) chemistry. *Current Science* **115**, 1334–41.

Singh IB (1973) Depositional environments in upper Vindhyan sediments in the Son Valley area. In *Geology of Vindhyanchal* (eds KS Valdiya, SB Bhatia and VK Gour), pp. 146–52. New Delhi: Hindustan Publishing (India).

Singh IB (1980) The Bijaigarh shale, Vindhyan system (Precambrian), India: an example of a lagoonal deposit. *Sedimentary Geology* **25**, 83–103.

Smith GA and Lowe DR (1991) Lahars: volcano-hydrologic events and deposition in the debris flow – hyperconcentrated flow continuum. In *Sedimentation in Volcanic Settings* (eds RV Fisher and GA Smith), pp. 59–70. SEPM (Society for Sedimentary Geology), Tulsa, Special Publication no. 45.

Soni MK, Chakraborty S and Jain VK (1987) Vindhyan Supergroup: a review. In *Purana Basins of Peninsular India (Middle to Late Proterozoic)* (ed. BP Radhakrishna), pp. 87–138. Geological Society of India, Bangalore, Memoir no. 6.

Srivastava P (2009) Trachyhystrichosphaera: an age-marker acanthomorph from the Bhander group, upper Vindhyan, Rajasthan. *Journal of Earth System Science* **118**, 575–82.

Srivastava P, Sinha R, Deep V, Singh A and Upreti N (2018) Micromorphology and sequence stratigraphy of the interfluve paleosols from the Ganga Plains: a record of alluvial cyclicity and paleoclimate during the Late Quaternary. *Journal of Sedimentary Research* **88**, 105–28.

Stow DAV, Huc AY and Bertrand P (2001) Depositional processes of black shales in deep water. *Marine and Petroleum Geology* **18**, 491–98.

Sur S, Schieber J and Banerjee S (2006) Petrographic observations suggestive of microbial mats from Rampur Shale and Bijaigarh Shale, Vindhyan basin, India. *Journal of Earth System Science* **115**, 61–66.

Swift DJP, Hudelson PM, Bernner RL and Thompson P (1987) Storm-deposited sandstone in upper cretaceous Mesa Verde group, Book Cliffs, Utah: role of prodelta shelf depositional system in the formation of foreland basin depositional sequence. *Sedimentology* **34**, 423–57.

Tandon SK, Pant CC and Casshyap SM (1991) *Sedimentary Basins of India-Tectonic Context*. Nainital: Gyanodaya Prakashan, 283 p.

Tirsgaard H and Sønderholm M (1997) Lithostratigraphy, sedimentary evolution and sequence stratigraphy of the Upper Proterozoic Lyell Land Group (Eleonore Bay Supergroup) of East and Northeast Greenland. *Geological Survey of Denmark* **178**, 60.

Tripathy GR and Singh SK (2015) Re–Os depositional age for black shales from the Kaimur Group, Upper Vindhyan, India. *Chemical Geology* **413**, 63–72.

Vail PR, Mitchum RM and Thomson S (1977) Seismic stratigraphy and global changes of sea level. Part 4: global cycles of relative changes of sea level. In *Seismic Stratigraphy- Applications to Hydrocarbon Exploration* (ed. CE Payton), pp. 83–98. American Association of Petroleum Geologists, Tulsa, Memoir no. 26.

Vallance JW (2000) Lahars. In *Encyclopedia of Volcanoes* (eds H Sigurdsson, BF Houghton, RS Mcnutt, H Rymer and J Stix), pp. 601–15. San Diego: Academic Press.

Van Wagoner, JC, Posamentier HW, Mitchum RM, Vail PR, Sard JF, Loutit TS and Hardenbol J (1988) An overview of sequence stratigraphy and key definitions. In *Sea Level Changes: An Integrated Approach* (eds CK Wilgus, BS Hastings, CGSC Kendall, HW Posamentier, CA Ross and JC Van Wagoner), pp. 39–45. SEPM (Society for Sedimentary Geology), Tulsa, Special Publication no. 42.

Verma RK (1991) *Geodynamics of the Indian Peninsula and Indian Plate Margins*. Rotterdam: AA Balkema, 357 p.

Walker RG and Plint AG (1992) Wave- and storm-dominated shallow marine systems. In *Facies Models: Response to Sea Level Change* (eds RG Walker and NP James), pp. 219–38. Geological Association of Canada, Newfoundland, GeoText 1.

Wani H and Mondal MEA (2011) Evaluation of provenance, tectonic setting and paleoredox conditions of the Meso-Neoproterozoic basins of the Bastar craton, Central Indian Shield: using petrography of sandstones and geochemistry of shales. *Lithosphere* **3**, 143–54.

Zecchin M and Catuneanu O (2013) High-resolution sequence stratigraphy of clastic shelves I: units and bounding surfaces. *Marine and Petroleum Geology* **39**, 1–25.

https://doi.org/10.1017/S0016756820001168 Published online by Cambridge University Press